

University of Windsor

Scholarship at UWindor

Electronic Theses and Dissertations

Theses, Dissertations, and Major Papers

1-1-1969

Non-linear theories in two-dimensional fully and partially cavitating flow.

Krishan Murari Agrawal
University of Windsor

Follow this and additional works at: <https://scholar.uwindsor.ca/etd>

Recommended Citation

Agrawal, Krishan Murari, "Non-linear theories in two-dimensional fully and partially cavitating flow." (1969). *Electronic Theses and Dissertations*. 6064.
<https://scholar.uwindsor.ca/etd/6064>

This online database contains the full-text of PhD dissertations and Masters' theses of University of Windsor students from 1954 forward. These documents are made available for personal study and research purposes only, in accordance with the Canadian Copyright Act and the Creative Commons license—CC BY-NC-ND (Attribution, Non-Commercial, No Derivative Works). Under this license, works must always be attributed to the copyright holder (original author), cannot be used for any commercial purposes, and may not be altered. Any other use would require the permission of the copyright holder. Students may inquire about withdrawing their dissertation and/or thesis from this database. For additional inquiries, please contact the repository administrator via email (scholarship@uwindsor.ca) or by telephone at 519-253-3000ext. 3208.

NON-LINEAR THEORIES IN TWO-DIMENSIONAL
FULLY AND PARTIALLY CAVITATING FLOW

by

Krishan Murari Agrawal

A Dissertation
Submitted to the Faculty of Graduate Studies through the Department
of Mathematics in Partial Fulfillment of the Requirements
for the Degree of Doctor of Philosophy
at the University of Windsor

Windsor, Ontario

1969

UMI Number: DC52631

INFORMATION TO USERS

The quality of this reproduction is dependent upon the quality of the copy submitted. Broken or indistinct print, colored or poor quality illustrations and photographs, print bleed-through, substandard margins, and improper alignment can adversely affect reproduction.

In the unlikely event that the author did not send a complete manuscript and there are missing pages, these will be noted. Also, if unauthorized copyright material had to be removed, a note will indicate the deletion.

UMI[®]

UMI Microform DC52631

Copyright 2008 by ProQuest LLC.

All rights reserved. This microform edition is protected against unauthorized copying under Title 17, United States Code.

ProQuest LLC
789 E. Eisenhower Parkway
PO Box 1346
Ann Arbor, MI 48106-1346

HRX 2250

APPROVED BY:

J. Heschilt

K. A. Fishbein

R. R. Meadley

X. Di. Omer

E. Cumberland

External Examiner

A. B. Smith

Supervisor

301805

DEDICATED TO

Jagdish Chandra Agrawal

my teacher

ABSTRACT

An analysis is made for fully and partially developed cavitating flow past a hydrofoil under the assumptions that the flow is irrotational, incompressible, steady and two-dimensional. The solutions are obtained by using conformal mapping theory and the Riemann-Hilbert technique. Firstly, three closed cavity models namely, modified-Riabouchinsky model, re-entrant jet model and Tulin's single spiral vortex model are compared and found in good agreement. In the second part of the present work a transverse gravity field is included in the analysis and its effects are discussed.

Finally, Wu's theory [44] is modified suitably for partially cavitating flow and some interesting results are obtained.

ACKNOWLEDGEMENTS

This work was carried out under the direction of Dr. A. C. Smith, to whom I am grateful for his expenditure of time and effort on my behalf.

I wish to thank also Rev. D. T. Faught for part-time teaching assistantships which contributed to my support.

The major portion of my support has come from a research assistantship derived from the Defense Research Board (Grant No. 9550-34 UG), and a bursary granted by the National Research Council. I am profoundly indebted to both of these bodies, and through them to the taxpayers of the Dominion of Canada.

TABLE OF CONTENTS

	Page
ABSTRACT	iv
ACKNOWLEDGMENTS	v
LIST OF TABLES	vii
LIST OF FIGURES	viii
NOMENCLATURE	xi
CHAPTER 1	
INTRODUCTION	1
CHAPTER II	
GENERAL THEORY	18
CHAPTER III	
COMPARISON OF THREE CLOSED CAVITY MODELS	24
CHAPTER IV	
CAVITATING FLOW IN THE PRESENCE OF GRAVITY	
(i) Steady, Plane Cavities in the Presence of Gravity	35
(ii) Analysis of Transverse Gravity Effect for a Symmetric Wedge	36
CHAPTER V	
FULLY AND PARTIALLY CAVITATING FLOW	
(i) Analysis of Fully Cavitating Flow using Modified Wu's Theory	50
(ii) Analysis of Partially Cavitating Flow using Modified Wu's Theory	55
APPENDIX A	64
APPENDIX B	68
REFERENCES	71
VITA AUCTORIS	104

LIST OF TABLES

	PAGE
1. Comparison of Riabouchinsky, Re-entrant Jet and Single Spiral Vortex Models; Cavity Length, Cavitation Number and Drag.	63

LIST OF FIGURES

	Page
1. Physical flow plane represented by cusped cavity model for fully cavitating flow.	75
2. Physical flow plane represented by Riabouchinsky model.	76
3. Physical flow plane represented by re-entrant jet model for fully cavitating flow.	77
4. Physical flow plane represented by Lavrent'ev model for fully cavitating flow.	78
5. Physical flow plane represented by Roshko's model for fully cavitating flow.	79
6. Physical flow plane represented by wake model for fully cavitating flow.	80
7. Physical flow plane represented by modified Riabouchinsky model.	81
8. Physical flow plane represented by single spiral vortex model for fully cavitating flow.	82
9. Physical flow plane represented by double spiral vortex model for fully cavitating flow.	83
10. Physical flow plane for fully cavitating flow (wedge).	84
11. Complex potential plane for fully cavitating flow (wedge).	85
12. Parametric plane for fully cavitating flow (wedge).	86
13. Flow showing body-cavity system.	87
14. Cavity length against cavitation number for single spiral vortex model for $\alpha = 15^\circ$ (wedge). Numerical results from Riabouchinsky model (*) and for re-entrant jet model (·) are also included.	88
15. Cavity length against cavitation number for single spiral vortex model for $\alpha = 30^\circ$. Numerical results for M. Riabouchinsky model (*) and re-entrant jet model (·) are also included.	89

	Page
16. Drag coefficient vs cavitation number for single spiral vortex model for $\alpha = 45^\circ$. The numerical results for re-entrant jet model (\bullet) are also included.	90
17. Drag coefficient vs cavitation number for single spiral vortex model for $\alpha = 90^\circ$. The numerical results for re-entrant jet model (\bullet) are also included.	91
18. The shape of upper spiral vortex for $\alpha = 15^\circ$ and $\sigma = 0.1$.	92
19. The effect of Froude number ($F^2 = 36$) on the cavity shape.	93
20. The effect of Froude number ($F^2 = 16$) on the cavity shape.	94
21. Physical flow plane for fully cavitating flow (flat plate).	95
22. Complex potential plane and parameter plane for fully cavitating flow (flat plate).	96
23. Physical flow plane for partially cavitating flow.	97
24. Complex potential plane and parameter plane for partially cavitating flow.	98
25. Lift coefficient vs cavitation number for fully cavitating flow (flat plate). Experimental results of Parkin (\ast) for $\alpha = 15^\circ$, Silbermann (\dagger) for $\alpha = 25^\circ$, and Dawson (\bullet) for $\alpha = 10^\circ$ are included.	99
26. Drag coefficient against cavitation number for fully cavitating flow (flat plate). Experimental results of Parkin (\ast) for $\alpha = 15^\circ$, Silbermann (\dagger) for $\alpha = 25^\circ$, and Dawson (\bullet) for $\alpha = 10^\circ$ are included.	100
27. Normalized cavity length against cavitation number. The horizontal line marks the transition between fully and partially cavitating regime.	101
28. Lift coefficient against cavitation number for flat plate, including both fully and partially cavitating regimes. Dashed lines represent Wu's results.	102

29. Drag coefficient against cavitation number for flat plate, including both fully and partially cavitating regimes. Dashed lines represent Wu's results.

NOMENCLATURE

- a = constant
- A_0 = the only non-zero power series coefficient
- A_j = constant, power series j th coefficient
- $K^2 = C$ = length of the cavity (from point of detachment to the rear of the cavity)
- $H(t)$ = solution of the homogeneous Hilbert problem
- K_1 = constant
- L_c = body-cavity configuration length
- l = wedge arm length
- p_0 = reference pressure at infinity
- p = pressure
- p_c = pressure in cavity
- q = magnitude of velocity
- q_0 = magnitude of velocity at infinity
- $Q(t)$ = solution of Riemann-Hilbert problem
- t = auxiliary half plane
- t_i = real t -plane coordinate
- W = complex potential
- x = horizontal coordinate in the physical plane
- y = vertical coordinate in the physical plane
- α = semi angle of wedge
- α_i = internal angle in polygon

- ζ = normalized conjugate complex velocity
- η = dummy variable
- θ = argument of complex velocity
- ρ = constant density of fluid
- σ = cavitation number
- τ = dummy variable
- ϕ = velocity potential
- ϕ_A, ϕ_D = velocity potential at points A,D
- ψ = stream function
- $\omega = \log \zeta$

CHAPTER I

INTRODUCTION

It is well known that a fully wetted body, immersed in an irrotational flow of an inviscid and incompressible fluid in which the velocity is continuous, experiences no drag. This is the well known paradox of d'Alembert. However, flows with drag can be obtained if tangential discontinuities in velocity are allowed across the 'free streamlines' which detach from the surface of the body. In 1868 Helmholtz first presented a two-dimensional theory of 'free streamlines', in which he defined the free streamline as the surface which divides the flow into two regions, stagnant and non-stagnant. Further properties of the free streamlines can be found in [27, p. 283-4].

Helmholtz, Kirchoff, Rayleigh and Bobileff considered the case of infinite wakes [17, p. 96-105] by assuming that the pressure in the wake region is the same as the pressure at infinity. However, this is unrealistic from the physical point of view. In real fluid flows a finite cavity and wake are always obtained and the pressure inside the cavity is less than the free stream pressure.

A fluid cavitates whenever the local pressure is equal to the vapour pressure of the fluid. In the case of high speed motion through a liquid, part of the wake becomes gaseous, and this part is called a 'cavity'. The length of the cavity depends upon a non-dimensional parameter called the cavitation number, defined as

$$\sigma = \frac{p_0 - p_c}{\frac{1}{2}\rho q_0^2} \quad (1.1)$$

where p_0 = some typical fluid pressure, in the following the pressure of the fluid at infinity

p_c = cavity pressure i.e., vapour pressure

q_0 = a typical fluid speed, in the following always the speed at infinity.

The magnitude of the cavitation number is an indication of the degree of cavitation or of the tendency to cavitate.

As Eisenberg [9] has mentioned, we can separate the cavities into two groups:

1. transient cavities or travelling cavities
2. steady state cavities

In the first case, also called bubble cavitation, we observe bubbles filled with vapour, which grow and diminish. The life cycle of such cavities is very small. A collection of these bubbles can sometimes give the impression of one big bubble, constant in shape and size. This can of course happen only in a nearly steady flow. In the second case we have one large bubble, constant in shape and size. The 'constant' shape and size must be considered as a time average, since in reality small oscillations of the cavity may occur. Such cavities commonly occur at the tips of propeller blades of ships and turbines. In the case of hydrofoils, whether used for stabilizing ships, or for supporting boats, the cavities are often of the ventilated type. This

means that air is introduced directly from the atmosphere or pumped through small holes on the foil, to low pressure areas on lifting surfaces or bodies operating in water. When ventilation occurs, areas which previously were experiencing low pressure are subjected to pressures approaching atmospheric pressure. This causes a significant change in the flow pattern and the force characteristic of the elements involved. Actually not very much is known about the circumstances which control the occurrence of either the first or second type of cavitation. Such questions relating to the inception of cavitation, will not be considered here. However, for further references see Eisenberg and Tulin [10, pp. 1 to 46].

Some of the most interesting cavities in nature are unsteady and three-dimensional. Here, however, we propose to discuss only certain questions about steady, two-dimensional cavities.

Since we are restricting ourselves to steady cavities, we may consider the boundary of the cavity as a streamline of the fluid along which the pressure is constant. With this assumption, the steady state cavity is amenable to mathematical treatment by means of the theory of free streamlines and complex variable.

For flows in which the free boundary is an interface between liquid and gas, as in cavitation, viscosity plays a minor role. We assume the motion to be irrotational.

In two-dimensional flows the condition of irrotationality takes the frequently useful intrinsic form [27, pp. 105-108]

$$\frac{\partial q}{\partial n} = \frac{q}{R} \quad (1.2)$$

where n denotes the normal to a streamline and R its radius of curvature; $\frac{\partial q}{\partial n}$ is positive when we move in towards the centre of curvature of a streamline. From Eq. (1.2) one concludes that the normal acceleration on a streamline is in the same direction as the curvature.

Cavitating flow may be further characterized by the following physical conditions, suggested by Brillouin [12, p. 322]:

(i) the free streamlines do not intersect the obstacle or each other.

(ii) The maximum flow speed is attained on the free boundary.

The first condition is imposed because of the continuity of the flow, while the second gives the basic physical assumption that a fluid cannot withstand tension, or more accurately, that the fluid cavitates when the pressure is less than or equal to the vapour pressure.

If we investigate the effect of positive cavitation number on the cavity shape, assuming steady plane flow and the Brillouin conditions, then we find from the convexity of the free streamlines, (a consequence of the second Brillouin condition and of Eq. (1.2)) that the curves must either intersect one another, extend to infinity downstream without intersection, or turn back to form a jet entering the cavity from behind. The first possibility is excluded for reasons of continuity, while the second can be proven self contradictory [13]. The

remaining possibility is the existence of a re-entrant jet which eventually strikes the body or the cavity wall. Therefore it follows that 'within the framework of the theory of irrotational non-selfintersecting flows, a steady cavitating flow with positive cavitation number is not possible' [12, p.323]. For the development of steady cavitating flows several models have been proposed to represent accurately the physical flow. Wu [42] has also explained that these models can represent more accurately the total force on a solid body as an integral of the local forces if properly chosen. The following models have been introduced up to the present to represent cavitating flow.

Physical Models

- (1) Cusped cavity model
- (2) Riabouchinsky model
- (3) Re-entrant jet model
- (4) Roshko model
- (5) Wake model
- (6) Modified-Riabouchinsky model
- (7) (i) Single spiral vortex model
(ii) Double spiral vortex model

In the mathematical formulation of these models the following conditions are satisfied:

- (i) the flow is steady, irrotational and two-dimensional,
- (ii) the pressure in the interior of the fluid is nowhere less than the cavity pressure,

or if $C_p = \frac{p-p_c}{\frac{1}{2}\rho q^2}$ then $C_p \geq 0$, where

p and q are the pressure and speed,

(iii) the static pressure of the uniform flow is greater than the cavity pressure, i.e. $\sigma > 0$,

(iv) the pressure is continuous across a free streamline,

(v) the detachment position is such that the curvature of the cavity and of the body is identical at the point of detachment (smooth detachment).

The main motivation of these models is to predict the forces acting on a body which are the complicated function of the body shape and cavitation number.

The main techniques applied in all these models in order to calculate the forces, cavity length, etc., are the theory of singular integral equations, analytic functions and conformal mappings.

In what follows, the flow pattern of each model will be outlined briefly:

The Cusped Cavity Model. The cusped cavity was first proposed by Brillouin [5, pp. 126-128]. This model of a finite cavity is characterized by a cusp at its trailing edge, Fig. (1). Since the maximum speed of the flow cannot be achieved on the free streamlines of a cusped cavity this model was rejected by Brillouin himself and in 1913, Villat showed that a symmetric cusped cavity behind a wedge is impossible in general [5, pp. 126-128, 145-146]. This model is therefore unsuited to the theory of cavitation, and is of questionable significance

altogether. However, in the presence of gravity a cusp at the rear of the cavity is possible, as discussed by Lenau and Street [237].

An explicit example of a flow past a curved obstacle was constructed by Lighthill [247]. By assuming that at the cusp the radius of curvature of both arms is zero, he found the general expression for the velocity potential at any cusp occurring naturally in potential flow. He constructed an example for a profile with rounded nose, cusped tail and constant velocity over the rear and gave expressions for the 'aerofoil' shape and velocity distribution.

The Riabouchinsky Model. This model was proposed by Riabouchinsky [33]. He solved the problem of flow past a plate normal to the main stream. A finite cavity is obtained by introducing an 'image' obstacle downstream of the real body. The principal advantage of this model is its mathematical simplicity. However, its generalization leads to very complicated algebra [46, p. 362-363]. The physical flow plane is shown in Fig. (2). In this model let AB be the given fixed boundary and A'B' its mirror image with respect to a vertical line. A uniform flow impinging on AB describes a Riabouchinsky cavity if AB and A'B' are both streamlines of the flow. The region enclosed by the fixed and free boundaries is the cavity. The cavitation number, or equivalently, the speed on the free streamlines, will of course depend on the distance between AB and its image A'B', and conversely, if the cavitation number is prescribed, the separation of AB and A'B' can be found.

The Re-entrant Jet Model. This representation, Fig. (3) of

cavitating flow was suggested by Prandtl and Wagner and was further extended by Gilbarç and Serrin [13], who mentioned similar work by

Efros. In this model we consider the mathematical idealization by allowing the jet to 'pass through' the obstacle, passing to a second sheet of the flow plane. The validity of this model lies in its closeness to experimental results and there seems little doubt, despite the non-physical feature of the second flow plane, that it provides an accurate representation of the cavitation phenomenon.

It may be shown that the jet is of finite width, and it is clear that the formation of the jet requires the flow to contain a stagnation point in its interior as well as on the obstacle (provided it is non-cusped). The only type of stagnation point consistent with a uniform flow at infinity and two free streamlines is one with two entering and two outgoing streamlines and it is supposed for this model that there is exactly one such point.

There is another interesting scheme which is very similar to the re-entrant jet model for cavitating flow which was proposed by Lavrentev [22, pp. 45-48].

In this representation it is assumed that the flow behind an arc τ_0 has two rings δ^\pm filled with liquid Fig. (4). The rings δ^\pm are bounded from outside by the curves τ^+ , τ^- and x-axis and from inside by τ_0 , τ_0^1 respectively. The flow problem is discussed under the following assumptions:

- (1) the basic flow is irrotational,
- (2) the flow in rings δ^\pm is irrotational or has constant

vorticity,

- (3) along the curve γ_0 , the velocity of the fluid in the ring has a given constant value,
- (4) along γ^+ , the velocity of the fluid in the ring must coincide with the velocity of the basic flow around the arc τ_0 augmented by the arcs γ^+ .

An explicit example in which τ_0 is the segment of a straight line is solved by the above theory by Pykhtev [32, 22, pp. 47].

Roshko's Model. This representation of a free streamline flow with the cavity pressure different from the free stream pressure was proposed by Roshko [34], in which the rear of the cavity is specified by two horizontal halflines A'I, B'I, the free streamline extending from A to A' and B to B' Fig. (5). The positions of A' and B', of course, depend on the cavitation number. In this model the base pressure in the wake (or cavity) near the body can take any assigned value. From a certain point in the wake (A¹ and B'), which can be determined from the theory, the flow downstream is supposed to be dissipated gradually from the assigned value to that of the stream in a strip (A'I and B'I) parallel to the free stream. Wu [42] discussed the case of cambered hydrofoils by representing the cavitating flow by this model.

The Wake Model. This model was proposed by Wu [44] and also independently by Fabula [11]. In this representation the flow is divided in two parts Fig. (6):

- (1) near-wake region,
- (2) far-wake region.

In the 'near-wake region' the flow is approximately described in the large by an equivalent potential flow such that along the wake boundary the pressure assumes a constant value. In the 'far-wake region' it then increases continuously from this underpressure to the given free streamline value in an infinite wake strip of finite width. One of the mathematical advantages of this model is its simplicity. Wu [45] has further generalized this model for an arbitrary profile. However, this model slightly over-predicts the results for partially and fully cavitating cases.

The Modified Riabouchinsky Model. The flow pattern is shown in Fig. (7). Clearly the Riabouchinsky cavity is only one of an infinite family of possible artificial models in each of which the cavity is closed by some fixed curves, i.e., plates. Poole [31] generalized the symmetric case and discussed some other aspects of this model. Plesset and Shaffer [30] generalized the Riabouchinsky model for a symmetric case by replacing the rear end of the cavity by a symmetrically placed wedge. Geurst [14] discussed the same flow by replacing the rear end of the cavity by a flat plate perpendicular to the main stream. Song [35] has shown that many mathematical models for cavitating flow are the special cases of a generalized Riabouchinsky model by assuming that the flow is symmetric about both the axes. Lenau and Street [23] employed this model to discuss the non-linear problem of a fully cavitating flow in the presence of a longitudinal gravity force.

As a matter of fact, none of these models predicts accurately the flow in the region of cavity collapse, which is highly turbulent.

Therefore none of the non-linear theories for finite cavities is exact. However, all these models have one essential feature in common: they are intended to give a satisfactory description of the flow near the body by making possible an adjustment of the base pressure and thereby removing a serious situation in the classical theory. Therefore, one should not expect that the solutions of the flow field will describe the wake far downstream. Fortunately, the flow at the rear of the cavity has very little influence on the flow about the body, and a preference for one model relative to another, can therefore, for engineering purposes, be fairly based on the consequent mathematical conveniences.

Spiral Vortex Model. Since we are going to use this model in further analysis we shall discuss this model in some detail.

Tulin [40] proposed a spiral vortex model in an attempt to describe the real cavity flow. He has explained why, in a real supercavitating flow, a wake actually exists behind the region of cavity collapse. This wake conducts a certain flow of momentum, the strength of which depends directly on the drag.

Generally, the displacement thickness of the wake behind the body decreases continuously to an asymptotic value equal to the momentum thickness; by displacement thickness δ we mean the thickness of the layer by which the potential flow is forced away from the boundary as a result of velocity reduction in the boundary layer; while the momentum thickness is based on the reduction of momentum due to frictional resistance of the body. Consequently, sufficiently far downstream the

momentum thickness is independent of the distance from the body. This relationship between the wake displacement thickness and momentum thickness is due to the important characteristics of the wake in its widening with increasing downstream distance by viscous and turbulent diffusion and in reduced velocity deficiency as it spreads. In the case of cavity-wake flow the wake starts, from the turbulent region just behind the cavity collapse and we can expect the same behaviour of the displacement thickness there. If we now take the x-axis in the direction of the undisturbed stream velocity u_0 and y-axis normal to it, with u and v the corresponding velocity components then the body drag must be equal to the net reduction of momentum flux in the x-direction far downstream. Since $\rho u dy$ is the mass flux across an element dy and $(u_0 - u)$ is the velocity reduction in x-direction, we have

$$\text{Drag } D' = \int_{\text{wake}} \rho u (u_0 - u) dy$$

Thus, the drag coefficient

$$C_D = \frac{D'}{\frac{1}{2} \rho u_0^2 C} = \frac{2}{C} \int_{\text{wake}} \frac{u}{u_0} \left(1 - \frac{u}{u_0}\right) dy$$

But we define the displacement thickness of the wake [46, pp. 19] as:

$$\delta = \int_0^{\infty} \left(1 - \frac{u}{u_0}\right) dy$$

Therefore, the asymptotic value of the trailing wake:

$$\frac{\delta(\infty)}{C} \sim \frac{C_D}{2} \quad (1.3)$$

where $\delta(\infty)$ is the asymptotic thickness and C is the chord length. Tulin [41, p. 1147] explained from Eq. (1.3) that a 'proper model' must neither ignore the wake nor involve too wide a trailing wake.

Keeping this in mind Tulin proposed two cavity models involving cavities which terminated in spiral vortices and are followed by trailing wakes, Figs. (8, 9). The single spiral vortex model involves a wake (or cavity) which is closed in the physical plane and a trailing wake which becomes thin downstream showing a behaviour similar to displacement thickness. The double spiral model which corresponds to a flow in a simply connected region in the complex potential plane is an attempt to take into account the approximate loss in pressure recovery which, of course, accompanies mixing at cavity collapse. The detailed discussion of these models can be found in [40,41].

In conclusion, we can classify these models in two main categories, open cavity and closed cavity models. In open cavity models, we have a thick wake, and the wake is bounded by curved plates or horizontal flat plates extending to infinity, while in the closed cavity models we have no trailing wake and the cavity is closed by a short plate, an image object, or a re-entrant jet where the object or the jet size may be proportional to the width of the thin wake. Though the various theories produce similar results regardless of the model used, experimental observations indicate that the use of the thick wake model is not physically justifiable [41].

Linearized Theory of Steady Cavity Flows.

In the linear theory we assume that the disturbances introduced by the body can be regarded as small. More specifically we assume that the velocity components can be written as $(u_0 + u, v)$ where u_0 is the undisturbed stream velocity with the x-axis taken in the direction of u_0 and u, v are the perturbation velocities. We regard $\frac{u}{u_0}, \frac{v}{u_0}$ as small quantities such that their squares and products and higher order terms can generally be neglected. In cavitating flow usually we linearize the velocity potential as well as the boundary shape. However, in the case of physical models we linearize neither velocity potential nor boundary shape. Since the main difficulty in seeking the exact solution stems from mapping an unknown curved contour, Song [36] has introduced the idea of quasi-linear process, in which he has shown that it is sufficient to linearize the boundary shape only or partially linearize the velocity potential.

Since many bodies giving rise to cavitation, are slender and are used in such a way that the angle of incidence of the fluid is small, it can be assumed that cavity flow problems admit a linearized treatment. It was only in 1953 that the first publication on linearized cavity flow problem appeared when Tulin [39] formulated a linearized theory for a symmetric wedge. This is more surprising, since thin airfoil theory had found, as much as thirty years earlier, many fruitful applications to all kinds of aerodynamic problems. This gap in classical hydrodynamics seems to have been filled somewhat now. Linearized

theory has been applied to lifting hydrofoils [29], both partially cavitating and supercavitating. These flow problems have practical importance because of their application to the cross-sections of propeller blades, whose thickness ratio, camber and the angle of incidence, are small. Supercavitating propellers have been designed using the results of the linearized theory. The effects of the walls or free surfaces on cavity flows, symmetric as well as unsymmetric have been considered by Ai [3] and Cohen and his co-workers [8]. The consideration of wall effects receives its importance largely from the fact, that cavity experiments are done in cavitation tunnels and it is, therefore, necessary to know to what extent the tunnel walls influence the observed flow field. Cascade flow has been treated also by linearized theory because of its importance in turbine design and as a first approximation to propellers.

A typical condition used in linearized theory is the one which requires that the cavity be closed. This condition, which results in determining the unknown cavity length, seems a reasonable one physically not mathematically. However, this condition is replaced by a boundedness condition by Song [36]. He applied this condition to a quasi-linear theory in which only the boundary profile is linearized.

It remains to consider the connection between linear and non-linear theories as a check on the validity of the linearized

theory. The answer to this question was given by Geurst [14] who showed that a modified Riabouchinsky model and re-entrant jet model possess the same first order expansion as the usual linearized (first order) theory.

Since Tulin's single spiral vortex model is close to physical reality, we have compared this particular model, in Chapter III, with two closed cavity models 1. the Riabouchinsky model, and 2. the re-entrant jet model. Then we have shown that the spiral vortex model possesses the same first order expansion as the linearized theory (first order). In Chapter IV we have solved a non-linear problem in presence of a transverse gravity field by placing a symmetric wedge in the flow. Besides comparing our results with the theoretical results available (linear as well as non-linear) we have tried to answer the following interesting questions posed by Tulin [41]:

- (a) Does a cavity of finite length exist for $\sigma = 0$ in presence of gravity?
- (b) Will positive lift, which deflects the cavity downwards, result in further shortening of the cavity, while negative lift cause its length to increase?
- (c) Does effect of gravity increase with decreasing cavitation number?
- (d) Is the effect of transverse gravity always to reduce the lift coefficient while the drag coefficient remains unchanged?

In Chapter V a non-linear problem of the fully and partially developed cavitating flow past an oblique flat plate is solved by the

Riemann-Hilbert technique. The flow is represented by Wu's open cavity model [44]. However, in our treatment Wu's model has been suitably modified by relaxing some of his assumptions. It is shown that through the Riemann-Hilbert technique the problem can be readily solved in closed form and the results are in good agreement with available experimental data.

CHAPTER II
GENERAL THEORY

We consider the steady, two-dimensional, irrotational flow of an inviscid, incompressible fluid past a fully cavitating symmetric wedge of angle 2α under the influence of transverse gravity. By fully cavitating flow we mean a cavity extending along the entire suction side and even beyond the trailing edge, while in partially cavitating flow the cavity terminates in front of the trailing edge. The term super-cavitating is, however, applied to fully cavitating flows regardless of whether the cavity is formed as a result of cavitation or ventilation.

Bernoulli's theorem can be written as:

$$p + \frac{1}{2} \rho q^2 + \rho g y = \text{Constant} \quad (2.1)$$

where p is the pressure, q is the speed of the fluid, y is the vertical distance between a point in the fluid and some reference elevation, ρ is the fluid density, and g is the acceleration due to gravity.

We define the cavitation number

$$\sigma = \frac{p_0 - p_c}{\frac{1}{2} \rho q_0^2} \quad (2.2)$$

and the Froude number

$$F = \sqrt{\frac{q_0^2}{g \ell}} \quad (2.3)$$

where ℓ is some characteristic length, and will be taken as the wedge length in what follows. When the Froude number is large enough, we

can neglect the effect of gravity.

If p_0 and q_0 are the pressure and speed at infinity where $y=0$, we have:

$$p + \frac{1}{2}\rho q^2 + \rho g y = p_0 + \frac{1}{2}\rho q_0^2 \quad (2.4)$$

If q_c is the fluid speed on the cavity free streamlines where $g = 0$, then from equations (2.2) and (2.4)

$$q_c = q_0(1+\sigma)^{1/2} \quad (2.5)$$

while in presence of gravity the fluid speed q can be expressed in terms of q_c and the Froude number by

$$\frac{q}{q_c} = \left(1 - \frac{1}{1+\sigma} \frac{1}{F^2} \frac{2y}{l}\right)^{1/2} \quad (2.6)$$

We use the customary method of introducing the velocity ζ as a new variable and then exploit the fact that the constant speed streamlines (in the absence of gravity), unknown in shape in the physical plane, become known curves in the hodograph plane.

The application of the theory of complex variable to two-dimensional flow problems, such as considered here, is too well known to need explanation. See for example [7], [17] and [27]. It suffices to define our symbols as follows:

$$z = x + iy$$

$$w = \phi + i\psi \quad (\text{complex potential})$$

$$\frac{dw}{dz} = \zeta = u - iv = q e^{-i\theta} \quad (\text{complex velocity}) \quad (2.7)$$

$$\omega = \log \frac{dw}{dz} = \log q + i(-\theta) \quad (2.8)$$

The ζ -plane is called the hodograph plane. We note, in passing that

[7]

$$\frac{\partial^2 v}{\partial x^2} + \frac{\partial^2 v}{\partial y^2} = \left(\frac{\partial^2 v}{\partial X^2} + \frac{\partial^2 v}{\partial Y^2} \right) |f'(z)|^2$$

where $Z = X + iY = f(z)$ is analytic. Hence if v is harmonic in the z -plane, it is also harmonic in the Z -plane, except where $f'(z) = 0$.

It is clear that any flow region bounded entirely by polygonal streamlines and constant speed streamlines is mapped into a region of the ζ -plane bounded by radial segments ($\theta = \text{constant}$) and circular arcs $q = \text{constant}$ and is mapped into a polygonal domain in the ω -plane.

Since the plane of the complex potential $w = \phi + i\psi$ is already a known polygonal region except for the specific locations of certain vertices, the flow problem is essentially solved if the mapping between the w -plane and the hodograph plane is known, with the appropriate boundary correspondence, for then $w(z)$ appears as the solution of the differential equation

$$\frac{dw}{dz} = \zeta \quad \text{or} \quad z = \int \frac{dw}{\zeta} \quad (2.9)$$

Thus the flow problem is reduced to that of conformal mapping between known regions. The principal tool is the Schwarz-Christoffel transformation which, through explicit mappings on a half-plane, expresses (2.9) in parametric form:

$$\zeta = \zeta(t) \quad w = w(t)$$

In general the Schwartz-Christoffel transformation is given by [7]:

$$\frac{dw}{dz} = A \prod_i (z - z_i)^{\alpha_i/\pi - 1} \quad (2.10)$$

where z_i is the z -plane coordinate related to the vertices of the polygon, and α_i is the corresponding internal angle in the w -plane; A is a constant.

The method of solution consists of two basic parts:

(a) Construction of conformal mapping between the physical plane and the complex potential plane and a parametric half plane.

(b) Solution in this plane of a well posed Riemann-Hilbert problem.

Towards this goal we can determine w as a function of the half-plane variable z by conformal mapping. We note that the argument of the complex velocity is known on the wedge while the magnitude of it is known along the free streamlines. Then by using the Riemann-Hilbert technique we construct $\omega(z)$ explicitly as a function of z and once $\omega(z)$ is known, the drag coefficient can be determined using Bernoulli's theorem.

The general solution of the Riemann-Hilbert problem in the upper-half plane is well known [19,20,26,36] and is outlined briefly in Appendix A. In this problem if the imaginary part of an analytic function $Q(z)$ is known at all points on the boundary i.e., on the real z -axis then $Q(z)$ is obtained in the entire upper-half plane from the formula:

$$Q(z) = \frac{1}{\pi} \int_{-\infty}^{\infty} \frac{\text{Im}[Q(\tau)]}{\tau - z} d\tau + \sum_{j=0}^{\infty} A_j z^j \quad (2.11)$$

where A_j are real constants and j represents all positive integers.

The addition of the infinite series on the right hand side of Eq. (2.11) occurs because $Q(t)$ is regular for all $|t| < \infty$ and real on the real axis.

Now, it remains to relate $\omega(t)$ to $Q(t)$ so that $\text{Im } Q(t)$ is known at every point on the real line.

We map the w -plane onto the t -plane so that the wedge is mapped onto a finite segment of the real axis, and the cavity boundary onto the remainder of the real axis. Then, we have boundary conditions along the real axis in terms of $\omega(t)$.

We can convert these conditions to those of the Riemann-Hilbert problem following the general method of solution reported by Cheng and Rott [6]. The original function $\omega(t)$ is alternately purely real or purely imaginary on the real axis, hence we construct an auxiliary function $H(t)$ which makes the quotient $Q(t) = \frac{\omega(t)}{H(t)}$ known on the entire real axis, and always imaginary as required. It is to be noted that $H(t)$ is a solution of the homogeneous mixed boundary value problem; i.e., the prescribed values of $\omega(t)$ are all zero along the real axis. The choice of the homogeneous solution $H(t)$ is quite arbitrary. In fact, it is shown in the Appendix B that any possible solution satisfying the Hölder condition is reducible to Eq. (2.11) with one value of $H(t)$.

A choice of $H(t)$ satisfying our requirement is (see Fig. 12):

$$H(t) = i [(t-t_1)(t-t_2)]^{1/2}, \quad t_1 < t_2 \quad (2.12)$$

where t_1 and t_2 correspond to the ends of the wedge.

Let

$$\text{Im}[H(t)] > 0$$

on the real axis for $t < t_1$, and select a branch cut on the real axis interval (t_1, t_2) so that $H(t)$ is single valued. Hence $\omega(t)$ can explicitly be constructed by the use of the Riemann-Hilbert solution where $\omega(t) = H(t)Q(t)$.

The unknowns of the flow can be determined by the following two conditions:

- (1) flow is uniform at infinity,
- (2) net source strength of the body-cavity combination must be zero; i.e., the cavity is closed.

These conditions are sufficient in every case to determine uniquely a set of physical and non-physical parameters of the flow.

CHAPTER III

COMPARISON OF THREE CLOSED CAVITY MODELS

In this chapter three closed cavity models are compared, namely: 1. modified Riabouchinsky model, 2. re-entrant jet model, 3. single spiral vortex model, and then, it is shown that the non-linear single spiral model possesses the same first order expansion as the usual linearized theory.

We consider the basic problem of flow past a symmetric wedge with a finite cavity in an unbounded fluid. In this chapter gravity effects are neglected. All constants are evaluated, and expressions for the pertinent results of the theory derived. We use the single spiral vortex model to represent the cavitating flow and the general theory of chapter II is applied.

Figure 10 depicts the physical plane (z -plane) for a wedge. The free streamlines of the cavity end in a pair of single spiral vortices D_1 and D_2 which are suggestive of the highly turbulent flow actually present there. The wedge angle is 2α and the undisturbed speed is $q_0 = u$ at infinity. The origin is chosen at the stagnation point with the x -axis parallel to the undisturbed flow.

Next consider the plane of the complex potential $w = \phi + i\psi$. The body cavity configuration appears as a closed slit in this plane because we prescribe $\theta(D_1) = \theta(D_2)$ and $\phi(D_1) = \phi(D_2)$, i.e., the images of D_1 and D_2 in the potential plane are identical. (See Figure 11)

The normalized conjugate complex velocity ζ and complex potential w are related by:

$$\zeta = \frac{1}{q_c} \frac{dw}{dz} = \frac{q}{q_c} e^{-i\theta} \quad (3.1)$$

So, we know either the direction or the magnitude of the complex velocity at each point on the wedge cavity boundary.

Further, we map the w -plane onto the upper half of the t -plane, by choosing the following correspondence between the planes:^{*}

$$\begin{aligned} \text{A: } w &= 0 & t &= 0 \\ \text{B: } w &= 1 & t &= +1 \\ \bar{\text{B: }} w &= e^{2\pi i} & t &= -1 \\ \text{D: } w &= \phi_D & t &= \infty \end{aligned}$$

The mapping is given by

$$t = K \left(\frac{w}{\phi_D - w} \right)^{1/2} \quad (3.2)$$

$$\text{where } K^2 = \phi_D - 1. \quad (3.3)$$

Now we introduce the new variable

$$\omega = \log \zeta = \log \frac{q}{q_c} + i(-\theta). \quad (3.4)$$

At the stagnation point, $\text{Re}(\omega)$ has a logarithmic singularity, and $\text{Im}(\omega)$ has a jump discontinuity. Then on the real axis of the t -plane we have the

*

The first part of the mapping makes the w -plane simply connected by

removing D to infinity in the \bar{w} -plane, where $\bar{w} = \frac{w(\phi_D - 1)}{\phi_D - w}$

Then the square root is taken, $t = \bar{w}^{1/2}$

following mixed boundary value problem:

$$\begin{aligned}
 \operatorname{Re}(\omega) &= 0 & -\infty < t < -1 \\
 \operatorname{Im}(\omega) &= \alpha & -1 < t < 0 \\
 \operatorname{Im}(\omega) &= -\alpha & 0 < t < 1 \\
 \operatorname{Re}(\omega) &= 0 & 1 < t < \infty
 \end{aligned} \tag{3.5}$$

Since ω is not imaginary for all real t , we have to construct an auxiliary function $H(t)$ such that $\frac{\omega(t)}{H(t)}$ is imaginary for all real t . In particular $H(t)$ is chosen so that,

$$\begin{aligned}
 \operatorname{Re}[H(t)] &= 0 & -\infty < t < -1 \\
 \operatorname{Im}[H(t)] &= 0 & -1 < t < +1 \\
 \operatorname{Re}[H(t)] &= 0 & 1 < t < \infty
 \end{aligned} \tag{3.6}$$

A function satisfying the above conditions is

$$H(t) = i[(t+1)(t-1)]^{1/2} \tag{3.7}$$

with a cut from $t = -1$ to $t = +1$ and where the branch of the square root is so chosen, that $H(t) \rightarrow it$ as $t \rightarrow \infty$.

Now following Cheng and Rott [6], we can convert these conditions to those of the Riemann-Hilbert Problem:

$$\begin{aligned}
 \operatorname{Im}\left[\frac{\omega(t)}{H(t)}\right] &= 0 & -\infty < t < -1 \\
 \operatorname{Im}\left[\frac{\omega(t)}{H(t)}\right] &= +\alpha[(1-t)(1+t)]^{-1/2} & -1 < t < 0 \\
 \operatorname{Im}\left[\frac{\omega(t)}{H(t)}\right] &= -\alpha[(1-t)(1+t)]^{-1/2} & 0 < t < 1 \\
 \operatorname{Im}\left[\frac{\omega(t)}{H(t)}\right] &= 0 & 1 < t < \infty
 \end{aligned} \tag{3.8}$$

The essential feature of this model is that there is a singularity at the centre of the spiral [40], which is the rear end of

the cavity, of the type:

$$\omega \sim (w - \Phi_D)^{-1/2} \quad (3.9)$$

Changing the variable we find that $\omega \sim t$ on the real axis as $t \rightarrow \infty$, hence we can conclude that $\frac{\omega(t)}{H(t)}$ must asymptotically become a constant. Therefore the series in Eq. (2.11) must reduce to a constant. Substituting the value of $\left[\frac{\omega(t)}{H(t)}\right]$ in Eq. (2.11) we have

$$\frac{\omega(t)}{H(t)} = \frac{\alpha}{\pi} \int_{-1}^0 \frac{d\eta}{(\eta-t)(1-\eta^2)^{1/2}} - \frac{\alpha}{\pi} \int_0^1 \frac{d\eta}{(\eta-t)(1-\eta^2)^{1/2}} + A_0 \quad (3.10)$$

or

$$\omega(t) = H(t) \left[\frac{\alpha}{\pi} \int_{-1}^0 \frac{d\eta}{(\eta-t)(1-\eta^2)^{1/2}} - \frac{\alpha}{\pi} \int_0^1 \frac{d\eta}{(\eta-t)(1-\eta^2)^{1/2}} + A_0 \right]. \quad (3.11)$$

$\omega(t)$ contains two unknowns, which can be determined from the following conditions:

(i) at infinity, which corresponds to $t = iK$, we have $q = q_0$ and $\theta = 0$, so

$$\begin{aligned} \operatorname{Re}[\omega(iK)] &= -\frac{1}{2} \log(1+\sigma) \\ \operatorname{Im}[\omega(iK)] &= 0 \end{aligned} \quad (3.12)$$

(ii) the closure of the cavity: we can formulate this condition mathematically from the fact that body and cavity form a streamline across which no fluid flows.

Let Γ be the curve enclosing body-cavity system, then the outflow is:

$$\int_{\Gamma} (u dy - v dx)$$

$$= \int_{\Gamma} \left(\frac{\partial \psi}{\partial y} dy + \frac{\partial \psi}{\partial x} dx \right) \quad (\text{see Fig. 13})$$

$$= [\psi]_{\Gamma}$$

$$= \left[\int_m w \right]_{\Gamma}$$

$$\text{But } [w]_{\Gamma} = \int_{\Gamma} \frac{dw}{dz} dz = \int_{\Gamma} \zeta dz$$

Now, we apply this condition to the single spiral vortex model in which single vortex termination involves a wake which is closed in the physical plane to the first order and is continuous across $\psi = 0$ in the ζ, ψ plane [41, p. 1148], we obtain,

$$\text{Im} \oint_{\Gamma} \zeta dz = 0 \quad (3.13)$$

It follows from (2.8) that if $|\zeta| \rightarrow \infty$ so does $|\omega|$ and if $|\zeta| \rightarrow 0$ then $|\omega| \rightarrow \infty$. Therefore, ζ and ω have the same singularities. Hence, one may write

$$\text{Im} \oint_{\Gamma} \zeta dz = \text{Im} \oint_{\Gamma} \omega dz = 0 \quad (3.14)$$

Since a source remains a source under conformal transformation [27, p. 212], it follows from [18, p. 173] that Eq. (3.14) can be expressed as:

$$\text{Im} \left[\frac{d\omega(t)}{dt} \right]_{t = iK} = 0 \quad (3.15)$$

Integrating Eq. (3.11), we obtain

$$\omega(t) = A_0 (1-t^2)^{1/2} - \frac{\alpha}{\pi} \log \left\{ \frac{(1-t^2)^{1/2} + 1}{(1-t^2)^{1/2} - 1} \right\} \quad (3.16)$$

Now applying the condition (3.12) to Eq. (3.16), we obtain

$$\log(1+\sigma) = 2 \left[\frac{\alpha}{\pi} \log \left\{ \frac{(1+K^2)^{1/2} + 1}{(1+K^2)^{1/2} - 1} \right\} - A_0 (1+K^2)^{1/2} \right] \quad (3.17)$$

and from Eq. (3.15) and Eq. (3.16) we obtain

$$A_0 = - \frac{2\alpha}{\pi K^2} \quad (3.18)$$

Combining Eq. (3.17) and (3.18) we have

$$\log(1+\sigma) = \frac{2\alpha}{\pi} \left[\log \left\{ \frac{(1+K^2)^{1/2} + 1}{(1+K^2)^{1/2} - 1} \right\} + \frac{2}{K^2} (1+K^2)^{1/2} \right] \quad (3.19)$$

The above expression gives the relation between cavitation number and cavity length. Since without great loss of accuracy we can use $L \approx \phi_D = K^2 + 1$ on substituting in (3.19) $K^2 = L - 1 = C$, we have

$$\log(1+\sigma) = \frac{2\alpha}{\pi} \left[\log \left\{ \frac{(1+C)^{1/2} + 1}{(1+C)^{1/2} - 1} \right\} + \frac{2}{C} (1+C)^{1/2} \right] \quad (3.20)$$

The flow field has been determined completely.

Expressions similar to Eq. (3.20) for the re-entrant jet model and for the modified Riabouchinsky model from [14] are as follows:

Re-entrant Jet Model

$$\log(1+\sigma) = \frac{4\alpha}{\pi} \log \left\{ \left(\frac{1}{C} \right)^{1/2} + (1 + \frac{1}{C})^{1/2} \right\} - 2 \log \left\{ 1 - \frac{2\alpha}{\pi} \left(\frac{1}{C} \right)^{1/2} (1 + \frac{1}{C})^{1/2} \right\} \quad (3.21)$$

Modified Riabouchinsky Model

$$\log(1+\sigma) = \frac{4\alpha}{\pi} \log \left\{ \left(\frac{1}{C} \right)^{1/2} + (1 + \frac{1}{C})^{1/2} \right\} + \log \left\{ \frac{4\alpha}{\pi} \left(\frac{1}{C} \right)^{1/2} (1 + \frac{1}{C})^{1/2} + \left(1 + \frac{16\alpha^2}{\pi^2} \frac{1}{C} (1 + \frac{1}{C})^{1/2} \right) \right\} \quad (3.22)$$

where α is the semi-wedge angle and c is the distance from the point of detachment to the cavity closure. Numerical results are shown in Table 1 and are in good agreement.

If we take a first approximation for small σ and α , then the relation (between σ and c) for the re-entrant jet model, the modified Riabouchinsky model and for Tulin's closed cavity is the same [14] and is given by the expression:

$$\sigma = \frac{4\alpha}{\pi} \left[(1/c)^{1/2} (1+c)^{1/2} + \log \left\{ (1/c)^{1/2} + (1+c)^{1/2} \right\} \right] \quad (3.23)$$

while the expression for small σ and α for Tulin's single spiral vortex model from Eq. (3.20) reduces to

$$\sigma = \frac{2\alpha}{\pi} \left[\log \left\{ \frac{(1+c)^{1/2} + 1}{(1+c)^{1/2} - 1} \right\} + 2/c (1+c)^{1/2} \right] \quad (3.24)$$

The Eqs. (3.23) and (3.24) are the same. These relations show that Tulin's single spiral vortex model possesses the same first order expansion as the linearized theory.

CALCULATION OF THE DRAG, WEDGE ARM LENGTH AND SHAPE OF THE FREE STREAMLINES

We have obtained an expression for $\omega(t)$ (Eq. (3.16)) valid in the entire upper half t -plane:

$$\omega(t) = -\frac{\alpha}{\pi} \left[i\pi - \log \left\{ \frac{1 - (1-t^2)^{1/2}}{1 + (1-t^2)^{1/2}} \right\} \right] + A_0 (1-t^2)^{1/2}$$

Here, we choose the 'correct' branch of the many-valued function

$$\log \left\{ \frac{(1-t^2)^{1/2} + 1}{(1-t^2)^{1/2} - 1} \right\}$$

by stipulating that the logarithm be real when t is purely imaginary; with this choice the function $\omega(t)$, as given by (3.16), will satisfy the boundary conditions (3.8).

On the real t -axis, taking the proper branch of $H(t)$ in the different regions, we obtain:

$$\omega(t) = -\frac{\alpha}{\pi} \left[-i\pi - \log \left\{ \frac{1 - (1-t^2)^{1/2}}{1 + (1-t^2)^{1/2}} \right\} \right] + A_0 (1-t^2)^{1/2}$$

$$\left(H(t) = (1-t^2)^{1/2} \right) \quad -1 \leq t \leq 0 \quad (3.25)$$

$$\omega(t) = -\frac{\alpha}{\pi} \left[+i\pi - \log \left\{ \frac{1 - (1-t^2)^{1/2}}{1 + (1-t^2)^{1/2}} \right\} \right] + A_0 (1-t^2)^{1/2}$$

$$\left(H(t) = (1-t^2)^{1/2} \right) \quad 0 \leq t \leq 1 \quad (3.26)$$

$$\omega(t) = -\frac{\alpha}{\pi} \left[-i\pi + 2i \arctan (t^2-1)^{1/2} \right] + i A_0 (t^2-1)^{1/2}$$

$$\left(H(t) = i(1+t^2)^{1/2} \right) \quad t \leq -1 \quad (3.27)$$

$$\omega(t) = -\frac{\alpha}{\pi} \left[i\pi - 2i \arctan (t^2-1)^{1/2} \right] - i A_0 (t^2-1)^{1/2}$$

$$\left(H(t) = -i(1+t^2)^{1/2} \right) \quad 1 \leq t \quad (3.28)$$

The force on the wedge is given by

$$F = -i \int_A^B (p-p_c) dz + i \int_A^{\bar{B}} (p-p_c) dz$$

From Eq. (3.2) we have

$$\frac{dw}{dt} = \frac{2K^2(K^2+1)t}{(t^2+K^2)^2} \quad (3.29)$$

and $(p-p_c) \frac{dz}{dw} = \frac{1}{2} \rho q_c^2 (e^{-w} - e^{\bar{w}})$ (See [27])

Thus,

$$F = -\frac{1}{2} \rho q_c^2 K^2(K^2+1) \left\{ \int_0^1 \left[e^{-w(t)} - e^{\bar{w}(t)} \right] \frac{t dt}{(t^2+K^2)^2} + \int_{-1}^0 \left[e^{-w(t)} - e^{\bar{w}(t)} \right] \frac{t dt}{(t^2+K^2)^2} \right\}$$

which reduces to

$$F = 2 \rho q_c^2 \sin \alpha K^2(K^2+1) \left\{ \int_0^1 e^{-A_0(1-t^2)^{1/2}} \left[\frac{1+(1-t^2)^{1/2}}{1-(1-t^2)^{1/2}} \right]^{d/\pi} \frac{t dt}{(t^2+K^2)^2} - \int_{-1}^0 e^{A_0(1-t^2)^{1/2}} \left[\frac{1-(1-t^2)^{1/2}}{1+(1-t^2)^{1/2}} \right]^{d/\pi} \frac{t dt}{(t^2+K^2)^2} \right\} \quad (3.30)$$

Hence the drag coefficient is:

$$C_{D_1} = \frac{F}{\frac{1}{2} \rho q_0^2 l} = \frac{2 \rho q_c^2 \sin \alpha K^2(K^2+1)}{\frac{1}{2} \rho q_0^2 l} (I_1 - I_2) \quad (3.31)$$

or

$$C_{D_1} = \frac{4 \sin \alpha K^2(K^2+1)}{l} [I_1 - I_2] (1+\sigma) \quad (3.32)$$

Where

$$I_1 = \int_0^1 e^{-A_0(1-t^2)^{1/2}} \left[\frac{1+(1-t^2)^{1/2}}{1-(1-t^2)^{1/2}} \right]^{d/\pi} \frac{t dt}{(t^2+K^2)^2} \quad (3.33)$$

and

$$I_2 = \int_0^1 e^{A_0(1-t^2)^{1/2}} \left[\frac{1-(1-t^2)^{1/2}}{1+(1-t^2)^{1/2}} \right]^{\alpha/\pi} \frac{t dt}{(t^2+K^2)^2} \quad (3.34)$$

Also, the length of one arm of the wedge is given by

$$\begin{aligned} l &= |Z_B - Z_A| \\ |Z_B - Z_A| &= \int_A^B |dz| = 2K^2(K^2+1) \int_0^1 e^{-A_0(1-t^2)^{1/2}} \left[\frac{1-(1-t^2)^{1/2}}{1+(1-t^2)^{1/2}} \right]^{\alpha/\pi} \frac{t dt}{(t^2+K^2)^2} \\ &= 2K^2(K^2+1) I_1 \end{aligned} \quad (3.35)$$

If we normalize the drag coefficients with respect to $2l \sin \alpha$ (width) we get the final expression for drag:

$$C_D = \frac{I_1 - I_2}{I_1} (1 + \sigma) \quad (3.36)$$

where I_1 and I_2 are given by Eq. (3.33) and (3.34).

In calculating the shape of the free streamlines we have to consider the value of $\omega(t)$ for the upper streamline when $t > 1$ (Eq. (3.28)) and for the lower streamline when $t < -1$ (Eq. (3.27)). On substituting these values of $\omega(t)$ into Eq. (2.9), we have the parametric representation of the free streamlines as:

$$\begin{aligned} x - x_0 &= \operatorname{Re}(Z - Z_0)_t \\ &= 2K^2(K^2+1) \int_{t_0}^t \operatorname{Cos} \left\{ \alpha + A_0(t^2-1)^{1/2} - \frac{2\alpha}{\pi} \tan^{-1}(t^2-1)^{1/2} \right\} \frac{t dt}{(t^2+K^2)^2} \end{aligned} \quad (3.37)$$

and

$$\begin{aligned} y - y_0 &= \operatorname{Im}(Z - Z_0)_t \\ &= (-1)^p 2K^2(K^2+1) \int_{t_0}^t \operatorname{Sin} \left\{ \alpha + A_0(t^2-1)^{1/2} - \frac{2\alpha}{\pi} \tan^{-1}(t^2-1)^{1/2} \right\} \frac{t dt}{(t^2+K^2)^2} \end{aligned} \quad (3.38)$$

For the upper streamline $p = +1$, $z_0 = z_B$, $t_0 = 1$, and $t > 1$

For the lower streamline $p = 2$, $z_0 = z_B$, $t_0 = -1$, and $t < -1$.

DISCUSSION OF RESULTS

In Figs. 14 and 15 the results for the cavity length vs cavitation number are plotted for $\alpha = 15^\circ$ and $\alpha = 30^\circ$. The results for the modified Riabouchinsky model and re-entrant jet model are also included. It is seen that all three closed cavity models (Tulin's single spiral, modified Riabouchinsky and re-entrant jet) are in excellent agreement.

Drag coefficients for $\alpha = 45^\circ$ and $\alpha = 90^\circ$ are reported in Figs. 16 and 17. The results for the Riabouchinsky model and the re-entrant jet model which are obtained [4] are also shown. It can be noted that the agreement is good, for, in the range of $.05 \leq \sigma \leq 2$, the deviation in the value of drag coefficient is less than 2%.

In Fig. 18 the shape of the upper streamline is shown for $\alpha = 15^\circ$ and $\sigma = 0.1$. It is interesting to note that when the integrand is zero in Eq. (3.37), i.e., $\frac{dx}{dt} = 0$, the streamline is vertical and when the integrand is zero in Eq. (3.38), i.e., $\frac{dy}{dt} = 0$, the streamline is horizontal and between successive zeros the integrands are alternatively positive and negative. This means that the streamlines are spiralling which is the essential feature of the model. Since the integrands are $O(t^{-3})$ for large t , we have only calculated the points on the streamline for t greater than the first few zeros of the integral. For larger t the remainder of either streamline shrinks to a point.

CHAPTER IV

STEADY, PLANE CAVITIES IN THE PRESENCE OF GRAVITY

In this chapter we propose to study the effects of gravity on a cavitating flow. The gravity may be considered as acting:

1. transversely, i.e., perpendicular to the direction of the flow at infinity, and
2. longitudinally, i.e., parallel to the direction of the flow at infinity.

The principal purpose of this chapter, however, is to study the transverse gravity effect on a flow past a symmetric wedge, with a finite trailing cavity. The actual magnitude of the effect of the gravity depends upon the Froude number and its orientation relative to the flow direction. The effect of the gravity may become important near free surfaces and in certain other applications. In general, the Froude numbers attained in water tunnel tests indicate a small gravitational effect. Only a few cavity theories have considered the influence of a gravity field.

Parkin [28] and Street [37] have presented linearized theories for flows in a transverse gravity field using an additional approximation in the boundary conditions. Street [38] has shown this approximation to be quantitatively equivalent to a first order solution in the small parameter $\frac{1}{F^2}$. In all these theories the assumption has been made that the ambient pressure is constant on each of the free streamlines, being

lower than the reference pressure at the forebody on the upper, and higher than this reference pressure on the lower, streamline.

The case of a longitudinal gravity field was studied by Acosta [2] and Lenau and Street [23]. Acosta [2] has developed a linearized theory by considering the flow past a symmetric wedge whereas Lenau and Street [23] have developed a non-linear theory by representing the cavitating flow by a modified Riabouchinsky model. They have found that for a gravity field pointing in the same direction as the flow the cavity is shortened, while for a gravity field pointing in a direction opposite to that of the flow, the cavity is lengthened. It is also interesting to note in these theories that after some critical value of the field strength, the trailing edge of the cavity becomes cusped rather than blunt. As mentioned by Tulin [4], real cavity flows involving longitudinal gravity fields are in most cases unsteady and the effect of unsteadiness can easily predominate.

The effect of gravity on the stability of the cavities is discussed by Chang-Yiwang [47].

ANALYSIS

The solution to our problem is based on an iterative procedure which employs the non-gravity solution as the initial trial solution. It is the same method as that used recently by Larock and Street [21]. Since we are using the same cavity model (single spiral vortex model) in the gravity case, it is very useful to know the properties of the non-gravity solution. There are two distinct advantages in using this

particular model:

1. we always know the location of the two free streamlines in the t -plane,
2. beyond some positive and negative values of t , $y(t)$ becomes essentially constant on each streamline because we are then in a spiralling vortex which terminates the cavity.

The former permits the referencing of information about the streamline to the known locations in the t -plane, independent of the effects of a gravity field. The latter allows us to avoid the numerical integration over the infinite intervals containing the free streamlines in the t -plane. Thus, let us denote these two values of $y(t)$ as y_L, y_U for the lower and upper streamlines respectively, where corresponding values of t are t_L and t_U . Then for $t \leq t_L$, $y(t) = y_L$; for $t \geq t_U$ $y(t) = y_U$.

In this problem the gravity acts parallel to the y -axis and in the negative direction. The formulation of the problem can now be completed by stating the boundary conditions. They are:

$$1. q = q_c \left(1 - \frac{1}{1+\sigma} \frac{1}{F^2} \frac{2y}{e}\right)^{1/2} \quad \text{on the cavity and as } z \rightarrow \infty$$

$$\log \frac{q_0}{q_c} \rightarrow -\frac{1}{2} \log(1+\sigma), \quad \int_m [\omega(t)]_{t=iK} = 0$$

2. The combination of the body and cavity must be closed.

The equivalent statement is that the net source strength must be zero [p.27].

3. Lastly, the flow cannot contain non-integrable singularities on the slit or have multiple values off the slit [5,p. 64].

Conditions 1. - 3. are sufficient to determine the flow field.

As in Chapter III we have the following boundary value

problem:

$$\left. \begin{aligned} \operatorname{Re}[\omega] &= \frac{1}{2} \log \left[1 - \frac{1}{1+\sigma} \frac{1}{F^2} \frac{2y(t)}{l} \right] & -\infty < t < -1 \\ \operatorname{Im}[\omega] &= \alpha & -1 < t < 0 \\ \operatorname{Im}[\omega] &= -\alpha & 0 < t < 1 \\ \operatorname{Re}[\omega] &= \frac{1}{2} \log \left[1 - \frac{1}{1+\sigma} \frac{1}{F^2} \frac{2y(t)}{l} \right] & 1 < t < \infty \end{aligned} \right\} (4.1)$$

In Eq. (4.1), F is a prescribed Froude number (see Fig. 1); α, σ, l and $y(t)$ are respectively, the semi-wedge angle, cavitation number, wedge length, and the ordinate of the free streamline for the gravity problem.

In order to apply the Riemann-Hilbert technique, we now form $\frac{\omega(t)}{H(t)}$ [p. 25-26]

as follows:

$$\left. \begin{aligned} \operatorname{Im} \left[\frac{\omega(t)}{H(t)} \right] &= -\frac{1}{2} \log \left[1 - \frac{1}{1+\sigma} \frac{1}{F^2} \frac{2y(t)}{l} \right] [(1+t)(t-1)]^{-1/2} & -\infty < t < -1 \\ \operatorname{Im} \left[\frac{\omega(t)}{H(t)} \right] &= \alpha [(1-t)(1+t)]^{-1/2} & -1 < t < 0 \\ \operatorname{Im} \left[\frac{\omega(t)}{H(t)} \right] &= -\alpha [(1-t)(1+t)]^{-1/2} & 0 < t < 1 \\ \operatorname{Im} \left[\frac{\omega(t)}{H(t)} \right] &= \frac{1}{2} \log \left[1 - \frac{1}{1+\sigma} \frac{1}{F^2} \frac{2y(t)}{l} \right] [(1+t)(t-1)]^{-1/2} & 1 < t < \infty \end{aligned} \right\} (4.2)$$

The Riemann-Hilbert power series will still give only one term as in Chapter III [p. 27]. Hence

$$\begin{aligned}
\omega(t) = H(t) \left\{ -\frac{1}{2\pi} \int_{-\infty}^{-1} \frac{\log \left[1 - \frac{1}{1+\sigma} \frac{1}{F^2} \frac{2y(\eta)}{\ell} \right] d\eta}{(\eta-t)(\eta^2-1)^{1/2}} \right. \\
+ \frac{\alpha}{\pi} \int_{-1}^0 \frac{d\eta}{(\eta-t)(1-\eta^2)^{1/2}} - \frac{\alpha}{\pi} \int_0^1 \frac{d\eta}{(\eta-t)(1-\eta^2)^{1/2}} \\
\left. + \frac{1}{2\pi} \int_1^{\infty} \frac{\log \left[1 - \frac{1}{1+\sigma} \frac{1}{F^2} \frac{2y(\eta)}{\ell} \right] d\eta}{(\eta-t)(\eta^2-1)^{1/2}} + A_0 \right\} \quad (4.3)
\end{aligned}$$

Here, two terms have been added to the non-gravity expression for $\omega(t)$, i.e., the integrals over $(-\infty, -1)$ and $(1, \infty)$.

In order to evaluate the extra integrals we will follow the Larock and Street method [21]. Recalling that $y(t) = y_L$ for $t \leq t_L$ and $y(t) = y_U$ for $t \geq t_U$, we obtain

$$\begin{aligned}
\int_{-\infty}^{-1} \frac{\log \left[1 - \frac{1}{1+\sigma} \frac{1}{F^2} \frac{2y(\eta)}{\ell} \right] d\eta}{(\eta-t)(\eta^2-1)^{1/2}} &= \log \left(1 - \frac{1}{1+\sigma} \frac{1}{F^2} \frac{2y_L}{\ell} \right) \\
&\cdot \int_{-\infty}^{t_L} \frac{d\eta}{(\eta-t)(\eta^2-1)^{1/2}} + \int_{t_L}^{-1} \frac{\log \left[1 - \frac{1}{1+\sigma} \frac{1}{F^2} \frac{2y(\eta)}{\ell} \right] d\eta}{(\eta-t)(\eta^2-1)^{1/2}}
\end{aligned}$$

Likewise,

$$\begin{aligned}
\int_1^{\infty} \frac{\log \left[1 - \frac{1}{1+\sigma} \frac{1}{F^2} \frac{2y(\eta)}{\ell} \right] d\eta}{(\eta-t)(\eta^2-1)^{1/2}} &= \log \left(1 - \frac{1}{1+\sigma} \frac{1}{F^2} \frac{2y_U}{\ell} \right) \\
&\cdot \int_{t_U}^{\infty} \frac{d\eta}{(\eta-t)(\eta^2-1)^{1/2}} + \int_1^{t_U} \frac{\log \left[1 - \frac{1}{1+\sigma} \frac{1}{F^2} \frac{2y(\eta)}{\ell} \right] d\eta}{(\eta-t)(\eta^2-1)^{1/2}}
\end{aligned}$$

The integrals over $(-\infty, t_L)$ and (t_U, ∞) can be evaluated exactly. The unknowns of the problem are the same as in the non-gravity case.

We can rewrite Eq. (4.3) as

$$\begin{aligned}
 \omega(t) = H(t) & \left\{ -\frac{1}{2\pi} \log\left(1 - \frac{1}{1+\sigma} \frac{1}{F^2} \frac{2y_L}{\ell}\right) \int_{-\infty}^{t_L} \frac{d\eta}{(\eta-t)(\eta^2-1)^{1/2}} \right. \\
 & + \frac{\alpha}{\pi} \int_{-1}^0 \frac{d\eta}{(\eta-t)(1-\eta^2)^{1/2}} - \frac{\alpha}{\pi} \int_0^1 \frac{d\eta}{(\eta-t)(1-\eta^2)^{1/2}} \\
 & + \frac{1}{2\pi} \log\left(1 - \frac{1}{1+\sigma} \frac{1}{F^2} \frac{2y_U}{\ell}\right) \int_{t_U}^{\infty} \frac{d\eta}{(\eta-t)(\eta^2-1)^{1/2}} - \frac{1}{2\pi} \int_{t_L}^{-1} \frac{\log\left(1 - \frac{1}{1+\sigma} \frac{1}{F^2} \frac{2y(\eta)}{\ell}\right) d\eta}{(\eta-t)(\eta^2-1)^{1/2}} \\
 & \left. + \frac{1}{2\pi} \int_1^{t_U} \frac{\log\left(1 - \frac{1}{1+\sigma} \frac{1}{F^2} \frac{2y(\eta)}{\ell}\right) d\eta}{(\eta-t)(\eta^2-1)^{1/2}} + A_0 \right\}. \quad (4.4)
 \end{aligned}$$

On the real t -axis, taking the proper branch of $H(t)$ in the different region, we obtain [pp. 30-31]:

$$\begin{aligned}
 \omega(t) = & -\frac{\alpha}{\pi} \left[-i\pi - \log\left\{ \frac{1-(1-t^2)^{1/2}}{1+(1-t^2)^{1/2}} \right\} \right] + A_0 (1-t^2)^{1/2} + J_\ell(t) \\
 & + \frac{i \log\left(1 - \frac{1}{1+\sigma} \frac{1}{F^2} \frac{2y_L}{\ell}\right)}{2\pi (1-t^2)^{1/2}} \left[\log\left\{ \frac{(1+t)^{1/2}(1-t_U)^{1/2} - (1-t)^{1/2}(1+t_U)^{1/2}}{(1+t)^{1/2}(1-t_U)^{1/2} + (1-t)^{1/2}(1+t_U)^{1/2}} \right\} \right. \\
 & \quad \left. - \log\{t - i(1-t^2)^{1/2}\} \right] \\
 & + \frac{i \log\left(1 - \frac{1}{1+\sigma} \frac{1}{F^2} \frac{2y_U}{\ell}\right)}{2\pi (1-t^2)^{1/2}} \left[\log\{t - i(1-t^2)^{1/2}\} - \log\left\{ \frac{(1+t)^{1/2}(1-t_U)^{1/2} - (1-t)^{1/2}(1+t_U)^{1/2}}{(1+t)^{1/2}(1-t_U)^{1/2} + (1-t)^{1/2}(1+t_U)^{1/2}} \right\} \right] \\
 & -1 \leq t \leq 0
 \end{aligned} \quad (4.5)$$

$$\begin{aligned}
\omega(t) = & -\frac{\alpha}{\pi} \left[i\pi - \log \left\{ \frac{1 - (1-t^2)^{1/2}}{1 + (1-t^2)^{1/2}} \right\} \right] + A_0 (1-t^2)^{1/2} + J_\ell(t) \\
& + \frac{i \log \left(1 - \frac{1}{1+\sigma} \frac{1}{F^2} \frac{2y_L}{L} \right)}{2\pi (1-t^2)^{1/2}} \left[\log \left\{ \frac{(1+t)^{1/2} (1-t_L)^{1/2} - (1-t)^{1/2} (1+t_L)^{1/2}}{(1+t)^{1/2} (1-t_L)^{1/2} + (1-t)^{1/2} (1+t_L)^{1/2}} \right\} \right. \\
& \quad \left. - \log \left\{ t - i(1-t^2)^{1/2} \right\} \right] \\
& + \frac{i \log \left(1 - \frac{1}{1+\sigma} \frac{1}{F^2} \frac{2y_U}{L} \right)}{2\pi (1-t^2)^{1/2}} \left[\log \left\{ t - i(1-t^2)^{1/2} \right\} - \log \left\{ \frac{(1+t)^{1/2} (1-t_U)^{1/2} - (1-t)^{1/2} (1+t_U)^{1/2}}{(1+t)^{1/2} (1-t_U)^{1/2} + (1-t)^{1/2} (1+t_U)^{1/2}} \right\} \right]
\end{aligned}$$

$$0 \leq t \leq 1 \quad (4.6)$$

where

$$J_\ell(t) = \frac{(1-t^2)^{1/2}}{2\pi} \left[\int_1^{t_U} \frac{\log \left(1 - \frac{1}{1+\sigma} \frac{1}{F^2} \frac{2y(\eta)}{L} \right) d\eta}{(\eta-t)(\eta^2-1)^{1/2}} - \int_{t_L}^{-1} \frac{\log \left(1 - \frac{1}{1+\sigma} \frac{1}{F^2} \frac{2y(\eta)}{L} \right) d\eta}{(\eta-t)(\eta^2-1)^{1/2}} \right]$$

$$(4.7)$$

$$\omega(t) = -\frac{\alpha}{\pi} \left[\mp i\pi^* + 2i \arctan (t^2-1)^{1/2} \right] \pm i A_0 (t^2-1)^{1/2} \pm i J(t) \pm$$

$$\begin{aligned}
& \frac{\log \left(1 - \frac{1}{1+\sigma} \frac{1}{F^2} \frac{2y_L}{L} \right)}{2\pi (t^2-1)^{1/2}} \left[\log \left\{ \frac{(1+t)^{1/2} (1-t_L)^{1/2} - (1-t)^{1/2} (1+t_L)^{1/2}}{(1+t)^{1/2} (1-t_L)^{1/2} + (1-t)^{1/2} (1+t_L)^{1/2}} \right\} \right. \\
& \quad \left. - \log \left\{ t \pm (t^2-1)^{1/2} \right\} \right] \\
& \pm \frac{\log \left(1 - \frac{1}{1+\sigma} \frac{1}{F^2} \frac{2y_U}{L} \right)}{2\pi (t^2-1)^{1/2}} \left[\log \left\{ \frac{(1+t)^{1/2} (1-t_U)^{1/2} + (1-t)^{1/2} (1+t_U)^{1/2}}{(1+t)^{1/2} (1-t_U)^{1/2} - (1-t)^{1/2} (1+t_U)^{1/2}} \right\} \right. \\
& \quad \left. + \log \left\{ t \pm (t^2-1)^{1/2} \right\} \right]
\end{aligned}$$

For $t \leq -1$ take (+) sign

For $t \geq 1$ take (-) sign

(4.8)

*
 (In the first term ($i\pi$) take (-) sign for $t \leq -1$ and (+) sign for $t \geq 1$)

where

$$J(t) = \frac{(t^2-1)^{1/2}}{2\pi} \left[\int_1^{t-\varepsilon} \frac{\log\left(1 - \frac{1}{1+\sigma} \frac{1}{F^2} \frac{2y(\eta)}{t}\right) d\eta}{(\eta-t)(\eta^2-1)^{1/2}} + \int_{t+\varepsilon}^{t_0} \frac{\log\left(1 - \frac{1}{1+\sigma} \frac{1}{F^2} \frac{2y(\eta)}{t}\right) d\eta}{(\eta-t)(\eta^2-1)^{1/2}} - \int_{t_L}^{-1} \frac{\log\left(1 - \frac{1}{1+\sigma} \frac{1}{F^2} \frac{2y(\eta)}{t}\right) d\eta}{(\eta-t)(\eta^2-1)^{1/2}} \right]$$

$$\text{For } t > 1 \quad (4.9)$$

$$J(t) = \frac{(t^2-1)^{1/2}}{2\pi} \left[\int_1^{t_0} \frac{\log\left(1 - \frac{1}{1+\sigma} \frac{1}{F^2} \frac{2y(\eta)}{t}\right) d\eta}{(\eta-t)(\eta^2-1)^{1/2}} - \int_{t_L}^{t-\varepsilon} \frac{\log\left(1 - \frac{1}{1+\sigma} \frac{1}{F^2} \frac{2y(\eta)}{t}\right) d\eta}{(\eta-t)(\eta^2-1)^{1/2}} - \int_{t+\varepsilon}^{-1} \frac{\log\left(1 - \frac{1}{1+\sigma} \frac{1}{F^2} \frac{2y(\eta)}{t}\right) d\eta}{(\eta-t)(\eta^2-1)^{1/2}} \right]$$

$$\text{For } t < -1 \quad (4.10)$$

As in the non-gravity case, we have two unknowns A_0 and K . Since boundary conditions at infinity ($t = i\infty$) still hold, the following integrals (using the notation of Larock and Street [21]) will be found useful:

$$I_1(\eta_1, \eta_2) = \int_{\eta_1}^{\eta_2} \frac{\log\left(1 - \frac{1}{1+\sigma} \frac{1}{F^2} \frac{2y(\eta)}{t}\right) d\eta}{(\eta^2+K^2)(\eta^2-1)^{1/2}}$$

$$I_2(\eta_1, \eta_2) = \int_{\eta_1}^{\eta_2} \frac{\log\left(1 - \frac{1}{1+\sigma} \frac{1}{F^2} \frac{2y(\eta)}{t}\right) d\eta}{(\eta^2+K^2)^2(\eta^2-1)^{1/2}}$$

A numerical investigation shows that the integrals (Eq. (4.4)) over the intervals (t_u, ∞) and $(-\infty, t_L)$ (these integrals represent the spiralling region of free streamlines) have very little effect on the other integrals. Therefore, in further calculations we will neglect these integrals.

The two equations for determining the unknowns which we had in the non-gravity case, ((1) and (2) p. 27) are:

$$-\frac{1}{2} \log(1+\sigma) = \frac{\alpha}{\pi} \log \left\{ \frac{(1+K^2)^{1/2} - 1}{(1+K^2)^{1/2} + 1} \right\} + \frac{(1+K^2)^{1/2}}{2\pi} \cdot \left\{ I_1(1, t_u) - I_1(t_L, -1) \right\} + A_0 (1+K^2)^{1/2} \quad (4.11)$$

$$\frac{-2\alpha}{\pi K (1+K^2)^{1/2}} + \frac{1}{2\pi} \left[-\frac{K}{(1+K^2)^{1/2}} \left\{ I_1(1, t_u) - I_1(t_L, -1) \right\} + 2K (1+K^2)^{1/2} \left\{ I_2(1, t_u) - I_2(t_L, -1) \right\} \right] - \frac{KA_0}{(1+K^2)^{1/2}} = 0 \quad (4.12)$$

From these two equations we can always find A_0, K for a given α, σ, t_L and t_u .

CALCULATIONS FOR WEDGE LENGTH, DRAG AND LIFT

Applying Eq. (2.8) and (2.9) the expression for the wedge arm length is:

$$l = \int_A^B |dz| = \int_0^1 2K^2(K^2+1) e^{-A_0(1-t^2)^{1/2}} J_0(t) \left[\frac{1+(1-t^2)^{1/2}}{1-(1-t^2)^{1/2}} \right]^{\alpha/\pi} \frac{t dt}{(t^2+K^2)^2}$$

The expression for the lift and drag is given by:

$$D + iL = -i \int_A^B (p - p_c) dz + i \int_A^{\bar{B}} (p - p_c) dz$$

From the Bernoulli's equation we have

$$\frac{p - p_c}{\frac{1}{2} \rho q_c^2} = \left[1 - \left(\frac{q}{q_c} \right)^2 - \frac{1}{1+\sigma} \frac{1}{F^2} \frac{2\gamma}{c} \right]$$

Defining the lift and drag coefficients, respectively, as

$$C_L = \frac{L}{\frac{1}{2} \rho q_c^2 c} \quad C_D = \frac{D}{\frac{1}{2} \rho q_c^2 c}$$

we have

$$\begin{aligned} C_D + iC_L &= -i/c \int_A^B \left[1 - \left(\frac{q}{q_c} \right)^2 - \frac{1}{1+\sigma} \frac{1}{F^2} \frac{2\gamma}{c} \right] dz \\ &\quad + i/c \int_A^{\bar{B}} \left[1 - \left(\frac{q}{q_c} \right)^2 - \frac{1}{1+\sigma} \frac{1}{F^2} \frac{2\gamma}{c} \right] dz \\ &= 2 \sin \alpha \left(1 - \frac{1}{1+\sigma} \frac{1}{F^2} \sin \alpha \right) + \frac{i}{c} \int_A^B \left(\frac{q}{q_c} \right)^2 dz - \frac{i}{c} \int_A^{\bar{B}} \left(\frac{q}{q_c} \right)^2 dz \\ &= 2 \sin \alpha \left(1 - \frac{1}{1+\sigma} \frac{1}{F^2} \sin \alpha \right) + \frac{i}{c} \int_0^1 e^{\bar{\omega}} \frac{d\bar{\omega}}{dt} - \frac{i}{c} \int_0^1 e^{\bar{\omega}} \frac{d\bar{\omega}}{dt} \\ &= 2 \sin \alpha \left(1 - \frac{1}{1+\sigma} \frac{1}{F^2} \sin \alpha \right) + \frac{i}{c} \left\{ 2 \int_0^1 e^{i\alpha + A_0(1-t^2)^{1/2}} J_0(t) \right. \end{aligned}$$

$$\cdot \left[\frac{1 - (1-t^2)^{1/2}}{1 + (1-t^2)^{1/2}} \right]^{\alpha/\pi} \frac{t K^2 (K^2 + 1) dt}{(t^2 + K^2)^2} + 2 \int_{-1}^0 e^{-i\alpha + A_0(1-t^2)^{1/2}} J_0(t)$$

$$\cdot \left[\frac{1 - (1-t^2)^{1/2}}{1 + (1-t^2)^{1/2}} \right]^{\alpha/\pi} \frac{t K^2 (K^2 + 1) dt}{(t^2 + K^2)^2} \left. \right\}$$

Let

$$I_C = \frac{2K^2(K^2+1)}{e} \int_{t_1}^t e^{A_0(1-t^2)^{1/2} + J_e(t)} \left[\frac{1-(1-t^2)^{1/2}}{1+(1-t^2)^{1/2}} \right]^{d/\pi} \frac{t dt}{(t^2+K^2)^2}$$

Then,

$$C_D = 2 \sin \alpha \left(1 - \frac{1}{1+\sigma} \frac{1}{F^2} \sin \alpha \right) + (I_{C_2} - I_{C_1}) \sin \alpha$$

$$C_L = (I_{C_1} + I_{C_2}) \cos \alpha$$

where I_{C_1} is the value of I_C with limits 0 to 1 and I_{C_2} is the value of I_C with limits -1 to 0.

The parametric representation of the free streamline is given

by:

$$z - z_0 = \int_{t_0}^t e^{-\omega(t)} \frac{dw}{dt} dt$$

where $\omega(t)$ is given by Eq. (4.8) and $t_0 = 1$ for the upper streamline and $t_0 = -1$ for the lower streamline.

Numerical Procedure

The iterative method which we have used in finding the numerical solution to the present problem is described in detail by Larock and Street [21]. The iterative procedure works in the following manner:

- (1) We determine all the parameters and the physical plane, especially $y(t)$ on the streamlines, from the non-gravity case (Chapter III) for a given K and α .
- (2) Using the input data from Step (1) where appropriate I_1, I_2 , (4.11) and A_0 , (4.12) are then computed. Then we determine $J(t)$ (4.10)

$y(t)$ (4.15) and $J(t)$ (4.7).

(3) Another gravity solution is obtained using the data from the step two as input data.

(4) Step (3) is repeated until the results of two successive iterations differ by less than some specified amount; at this point we stop the calculations and the gravity solution is obtained.

The method just described is direct and simple to apply. However, there is one drawback to this method, namely, that it is very time-consuming. Even computation of one iteration takes a considerable time on a high speed computer.

First, $y(t)$, or some approximation to $y(t)$, is assumed to be known as a continuous function of t . The functions $J(t)$ and $J'(t)$ must also be determined as continuous functions of t since they occur in various integrands. It is not possible to compute the values of these functions for all t because it would be a very tedious and expensive process. Therefore, $y(t)$, $J(t)$ and $J'(t)$ are computed for a selected, finite number of points t_i . Then by using interpolation methods these functions are approximated between the points t_i .

In numerical calculations, proper care must be taken at the singularities of the integrands, even though a singularity is integrable.

In Eq. (4.10), valid for $t < -1$, the integrand over the interval $(1, t_u)$ has a square root singularity at 1. We treat the remainder of the integrand as a constant over the interval $(1, 1+\epsilon)$ and integrate the singular portion:

$$\begin{aligned}
\int_1^{t_U} \frac{\log \left[1 - \frac{1}{1+\sigma} \frac{1}{F^2} \frac{2y(\eta)}{\ell} \right] d\eta}{(\eta-t)(\eta^2-1)^{1/2}} &= \frac{\log \left[1 - \frac{1}{1+\sigma} \frac{1}{F^2} \frac{2y_0}{\ell} \right]}{2(1-t)} \int_1^{1+\epsilon} \frac{d\eta}{(\eta-1)^{1/2}} \\
&+ \int_{1+\epsilon}^{t_U} \frac{\log \left[1 - \frac{1}{1+\sigma} \frac{1}{F^2} \frac{2y(\eta)}{\ell} \right] d\eta}{(\eta-t)(\eta^2-1)^{1/2}} \\
&= \frac{\log \left[1 - \frac{1}{1+\sigma} \frac{1}{F^2} \frac{2y_0}{\ell} \right]}{2(1-t)} \cdot 2\epsilon^{1/2} + \int_{1+\epsilon}^{t_U} \frac{\log \left[1 - \frac{1}{1+\sigma} \frac{1}{F^2} \frac{2y(\eta)}{\ell} \right] d\eta}{(\eta-t)(\eta^2-1)^{1/2}}
\end{aligned}$$

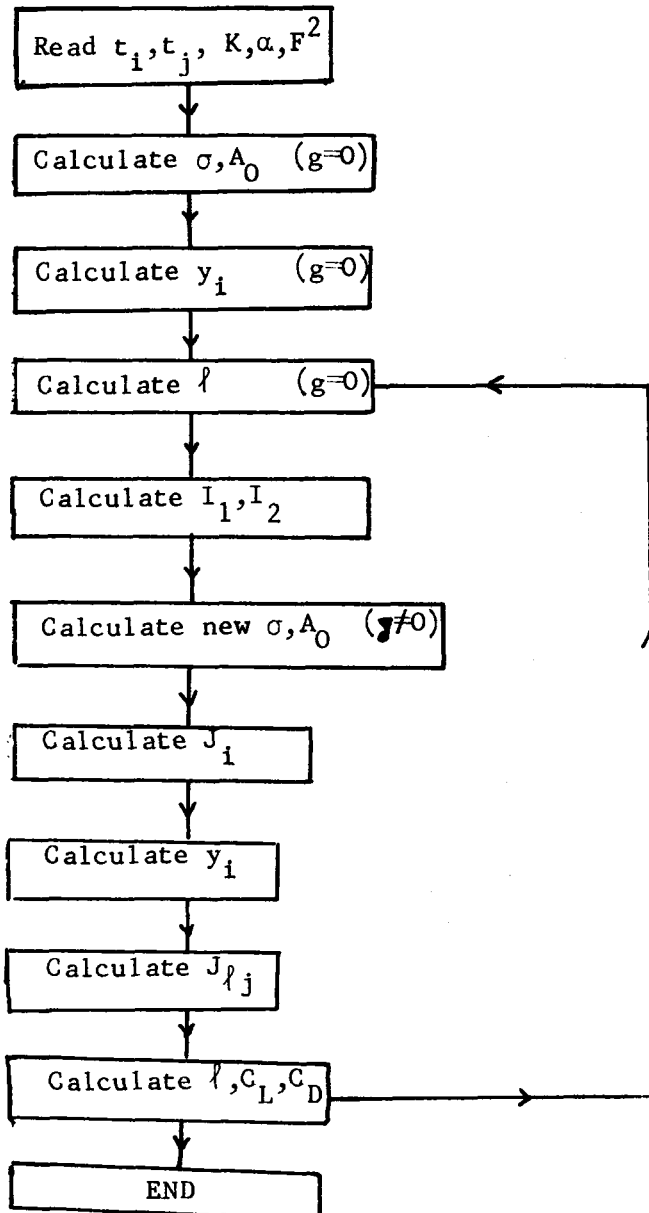
For a specified t and ϵ , the term can now be computed numerically.

So long as $0 < \epsilon < 1$, the specific choice of ϵ is not important.

Likewise, we can treat the integral over $(t_L, -1)$.

As pointed out in Chapter III, the points where the streamlines are vertical at the end of the cavity can be found as a function of t by finding the first zero of the integrand of Eq. (3.38). We call this point t_U . Since we are considering a symmetric flow in the non-gravity case, the value of t_L will be the negative of t_U . The roots which make the integrand zero can be found quite simply by a bisection procedure.

FLOW CHART



DISCUSSION

Figures 19 and 20 show the effect of the Froude number on the cavity shape. The cavity for the gravity solution is smaller and lies entirely within the gravity-free case. Also, the change in the drag coefficient from the non-gravity case to the gravity case is small.

From the present theory there results a negative lift coefficient. Intuitively, it seems that it will become positive only when the cavity is so short that its downward pulling effect is balanced by the buoyant force of the free body.

As discussed by Larock and Street (21) and Parkin (28) it can be shown in the present case also that the effect of the gravity increases with decreasing cavitation number. This simply means that longer cavities are more affected by the gravity than the short ones.

CHAPTER V

ANALYSIS OF FULLY CAVITATING FLOW

We consider the fully cavitating flow past a flat plate inclined at an angle α to an infinite parallel, fluid flow. We assume a reference system with the origin at the stagnation point on the plate and with the x-axis parallel to the undisturbed flow. The physical flow plane is shown in Fig. 21.

We shall discuss the flow under the following assumptions

1. the flow separates smoothly from the edges A and B of the plate,

2. the wake is bounded by two smooth free streamlines, each of which consists of two different parts. The first part, on which the pressure is constant, starts from the points of separation down to certain points c and c' and encloses the cavity of the 'near-wake' region. On the remaining part of the free streamlines, the pressure increases continuously from p_c to the main stream pressure p_∞ ,

3. the free streamlines are parallel to the main flow at points at infinity E and E',

4. the flow is irrotational outside the wake,

5. the potential ϕ and the flow inclination θ have respectively the same value at c and c' :

$$\phi_c = \phi_{c'}, \quad \text{and} \quad \theta_c = \theta_{c'}$$

i.e.,
$$w_c = w_{c'} \quad \text{and} \quad \zeta_c = \zeta_{c'}$$

However, in the present analysis we are not assuming the 'hodograph-slit condition'. Wu [44] has assumed the 'hodograph-slit condition' in order to map the variable pressure parts of the two free streamlines in the velocity plane.

We begin by mapping the complex potential plane $w = \phi + i\psi$ onto the upper-half of an auxiliary t -plane (Fig.22) by choosing the following correspondence:

$$\begin{aligned} D: w = 0 & \quad t = 0 \\ B: w = e^{2\pi i} & \quad t = -1 \\ C: w = \phi_c & \quad |t| = \infty \end{aligned}$$

The mapping is then given by

$$t = K \left(\frac{w}{\phi_c - w} \right)^{1/2} \quad (5.1)$$

where $K = [\phi_c - 1]^{1/2}$ and t_A are unknowns.

The points at infinity E and E' are carried by the mapping (5) onto the point $t = iK$.

We have then the following boundary value problem on the real t -axis for $\omega(t)$:

$$\left. \begin{aligned} \operatorname{Re}(\omega) &= 0 & -\infty < t < -1, t_A < t < \infty \\ \operatorname{Im}(\omega) &= \alpha & -1 < t < 0 \\ \operatorname{Im}(\omega) &= \alpha - \pi & 0 < t < t_A \end{aligned} \right\} \quad (5.2)$$

This problem can be converted to the ordinary Riemann-Hilbert problem for the function $\frac{\omega(t)}{H(t)}$, where

$$H(t) = -i[(t - t_A)(t + 1)]^{1/2}$$

is a homogeneous solution of the mixed boundary value problem [6]. It

is to be noted that this function $H(t)$ is not unique, but the solution is independent of the particular choice of $H(t)$ [Appendix B].

Then we have,

$$\begin{aligned} \int_m \left[\frac{\omega(t)}{H(t)} \right] &= 0 \quad -\infty < t < -1, \quad t_A < t < \infty \\ \int_m \left[\frac{\omega(t)}{H(t)} \right] &= \alpha \left[(t_A - t)(t+1) \right]^{-\frac{1}{2}} \quad -1 < t < 0 \\ \int_m \left[\frac{\omega(t)}{H(t)} \right] &= -(\pi - \alpha) \left[(t_A - t)(t+1) \right]^{-\frac{1}{2}} \quad 0 < t < t_A \end{aligned} \quad (5.3)$$

From the assumption (5, page 50) it follows that $\frac{\omega(t)}{H(t)} \rightarrow 0$ as $|t| \rightarrow \infty$. Therefore $A_j = 0$ in Eq. (2.11) and we obtain the following equation:

$$\omega(t) = H(t) \left\{ \frac{\alpha}{\pi} \int_{-1}^{t_A} \frac{d\eta}{(\eta-t)[(t_A-\eta)(1+\eta)]^{\frac{1}{2}}} - \int_0^{t_A} \frac{d\eta}{(\eta-t)[(t_A-\eta)(1+\eta)]^{\frac{1}{2}}} \right\} \quad (5.4)$$

where, of course, the Cauchy principal value must be taken at $\eta = t$.

Integrating Eq. (5.4) we obtain

$$\omega(t) = i\alpha + \log \left\{ \frac{(t_A - t)^{\frac{1}{2}} - [t_A(1+t)]^{\frac{1}{2}}}{(t_A - t)^{\frac{1}{2}} + [t_A(1+t)]^{\frac{1}{2}}} \right\} \quad -1 \leq t \leq t_A \quad (5.5)$$

and

$$\omega(t) = i\alpha - \log \left\{ \frac{-2t_A + t(1-t_A) + 2i\epsilon [t_A(1+t)(t-t_A)]^{\frac{1}{2}}}{t(1+t_A)} \right\} \quad (5.6)$$

where

$$\epsilon = +1 \quad \text{for } t > t_A$$

$$\epsilon = -1 \quad \text{for } t < -1$$

The two unknowns of the problem, K and t_A , can be determined by the condition that the flow be undisturbed at infinity. Then for $t = iK$ we have $q = U$ and $\theta = 0$, whence

$$\left. \begin{aligned} \operatorname{Re}[\omega(iK)] &= \log \frac{U}{q_c} = -\frac{1}{2} \log(1+\sigma) \\ \operatorname{Im}[\omega(iK)] &= 0 \end{aligned} \right\} \quad (5.7)$$

Applying the conditions of Eq. (5.7) to equation (5.5), we have

$$\left. \begin{aligned} \frac{1}{2} \log(1+\sigma) &= \beta_1 I_1 - \beta_2 I_2 \\ \alpha &= \beta_1 I_2 + \beta_2 I_1 \end{aligned} \right\} \quad (5.8)$$

where

$$\beta_r = (-1)^r \left[\frac{\delta^2}{2} - (-1)^r (K^2 + t_A) \right]^{\frac{1}{2}}, \quad r=1,2$$

$$I_r = \frac{\beta_r}{2\delta^2} (-1)^r \log \left(\frac{\beta_r^2 + \alpha_r^2}{\beta_1^2 + \alpha_1^2} \right) + \frac{1}{\delta^2} \left(\frac{\beta_1}{\beta_2} \right)^{r-1} \beta_2 \left[\pi - \tan^{-1} \frac{\alpha_2}{\beta_2} \right], \quad r=1,2$$

$$\delta^2 = \left[(K^2 + t_A)^2 + K^2 (1 - t_A)^2 \right]^{\frac{1}{2}}$$

$$P_r = \beta_5 - (-1)^r \beta_3 t_A^{\frac{1}{2}}, \quad r=1,2$$

$$Q_r = \beta_6 - (-1)^r \beta_4 t_A^{\frac{1}{2}}, \quad r=1,2$$

$$\beta_r = (-1)^r \left[\frac{1}{2} (1 + K^2)^{\frac{1}{2}} + \frac{1}{2} (-1)^r \right]^{\frac{1}{2}}, \quad r=3,4$$

$$\beta_r = \left[\frac{1}{2} (t_A + K^2)^{\frac{1}{2}} + \frac{t_A}{2} (-1)^r \right]^{\frac{1}{2}}, \quad r=5,6$$

and

$$\tau = \begin{cases} \tan^{-1} \frac{\theta_1}{P_1} & P_1 > 0 \\ \pi/2 & P_1 = 0 \\ \pi + \tan^{-1} \frac{\theta_1}{P_1} & P_1 < 0 \end{cases}$$

Equation (5.8) has been solved in terms of α and σ by numerical cross-plotting.

We shall normalize our results with respect to free stream-line speed q_c in our numerical treatment, i.e., we shall assume, without loss of generality, $q_c = 1$.

From Eq. (2.8) and (2.9) we obtain

$$z_A - z_B = \int_{-1}^{t_A} e^{-\omega(t)} \frac{d\omega}{dt} dt \quad (5.9)$$

where

$$\frac{d\omega}{dt} = \frac{2K^2(K^2+1)t}{(t^2+K^2)^2}$$

The length of the plate is then

$$l = |z_A - z_B| = \frac{4K^2(K^2+1)}{1+t_A} \int_{-1}^{t_A} \left\{ t_A - \left(\frac{1-t_A}{2}\right)t + [t_A(t_A-t)(t+1)]^{1/2} \right\} \frac{dt}{(t^2+K^2)^2} \quad (5.10)$$

where K , t_A are given by Eq. (5.8) in terms of α and σ .

The lift and drag coefficients are given by:

$$C_D = \frac{D}{\frac{1}{2} \rho q_c^2 l} = (1 + I_c) \sin \alpha \quad (5.11)$$

$$C_L = \frac{L}{\frac{1}{2} \rho q_c^2 l} = (1 + I_c) \cos \alpha \quad (5.12)$$

where

$$I_c = \frac{4K^2(K^2+1)}{(1+t_A)} \int_{-1}^{t_A} \left\{ -t_A + \left(\frac{1-t_A}{2}\right)t + [t_A(t_A-t)(1+t)]^{1/2} \right\} \frac{dt}{(t^2+K^2)^2} \quad (5.13)$$

Numerical results are discussed in the last part of the chapter.

ANALYSIS OF PARTIALLY CAVITATING FLOW

As described in Chapter II (p. 18), the partially cavitating flow is defined by a configuration in which the cavity or 'near wake' region extends from the leading edge A to a point C upstream of the trailing edge B. We assume a reference system centered at the stagnation point D on the plate and with the x-axis parallel to the plate (see Fig. 23).

We shall discuss the flow under the following assumptions:

1. The upper streamline, detaching from the leading edge, is divided into two regions: a region of constant pressure from A to C, enclosing the cavity, and a region from C to E where pressure increases smoothly from p_c to p_0 . Along the lower streamline, detaching from the trailing edge, the pressure is continuously increasing to p_0 and there is no region of constant pressure.

2. There exists a point \bar{B} on the upper streamline where the potential ϕ is the same as at B, and the upper streamline is parallel to the plate from C to \bar{B} . Wu [44] has assumed B is exactly above \bar{B} .

Moreover, conditions (1), (3), and (4) of the fully cavitating case (p. 50) also are assumed here. However, we shall not take the circulation around the cavity explicitly into account, and again no hodograph-slit

condition is assumed here [44].

As in the fully cavitating case, we begin by mapping the complex potential plane w onto the upper half of an auxiliary t -plane (Fig. 24) by choosing the following correspondence:

$$\begin{aligned} D: w = 0 & \quad t = 0 \\ A: w = 1 & \quad t = 1 \\ B: w = \phi_B & \quad |t| = \infty \end{aligned}$$

The mapping is given by

$$t = K \left[\frac{w}{\phi_B - w} \right]^{1/2} \quad (5.14)$$

where $K^2 = \phi_B - 1$ and t_c are unknowns.

Here, we have the following mixed boundary value problem on the real t -axis for the function $\omega(t)$,

$$\left. \begin{aligned} \Im_m(\omega) &= 0 & -\infty < t < 0, \quad t_c < t < \infty \\ \Im_m(\omega) &= -\pi & 0 < t < 1 \\ \operatorname{Re}(\omega) &= 0 & 1 < t < t_c \end{aligned} \right\} \quad (5.15)$$

Choosing the homogeneous solution

$$H(t) = -i[(t-1)(t_c-t)]^{1/2} \quad (5.16)$$

the function $\frac{\omega(t)}{H(t)}$ satisfies the following boundary conditions on the real axis:

$$\left. \begin{aligned} \Im_m \left[\frac{\omega(t)}{H(t)} \right] &= 0 & -\infty < t < 0, \quad t_c < t < \infty, \quad 1 < t < t_c \\ \Im_m \left[\frac{\omega(t)}{H(t)} \right] &= -\pi [(1-t)(t_c-t)]^{-1/2} & 0 < t < 1 \end{aligned} \right\} \quad (5.17)$$

As before, $\frac{\omega(t)}{H(t)} \rightarrow 0$ for $|t| \rightarrow \infty$, therefore $A_j = 0$ in Eq. (2.11) and we obtain the following equation for $\omega(t)$:

$$\omega(t) = H(t) \int_0^1 \frac{d\eta}{(t-\eta)[(1-\eta)(t_c-\eta)]^{1/2}} \quad (5.18)$$

Integrating equation (5.18) we obtain

$$\omega(t) = \log [t(t_c-1)] - \log [t(1+t_c) - 2t_c - 2t_c^{1/2} H(t)] \quad (5.19)$$

where the proper branch of the many-valued function $H(t)$ must be taken in the different regions of the real t -axis [6].

Again, the unknowns K and t_c can be determined from the condition at $t = ik$ ($Z = \infty$):

$$\omega(ik) = \log \left(\frac{1}{1+\sigma} \right)^{1/2} - i\alpha \quad (5.20)$$

Separating real and imaginary parts, we obtain

$$\left. \begin{aligned} \sigma &= \frac{(2t_c + 2x_1 t_c^{1/2})^2 + [2t_c^{1/2} \gamma_1 - K(1+t_c)]^2}{K^2 (t_c - 1)^2} \\ \alpha &= \frac{\pi}{2} + \arctan \left[\frac{2\gamma_1 t_c^{1/2} - K(1+t_c)}{2t_c + 2x_1 t_c^{1/2}} \right] \end{aligned} \right\} \quad (5.21)$$

where,

$$\left. \begin{aligned} x_1 &= \left[\frac{t_c - K^2}{2} + \frac{1}{2} \left\{ (K^2 + t_c)(K^2 + 1) \right\}^{1/2} \right]^{1/2} \\ \gamma_1 &= \frac{-K(t_c + 1)}{2x_1} \end{aligned} \right\} \quad (5.22)$$

These equations have been solved for t_c and K by numerical cross-plotting, as in the previous case.

The length of the plate is now given by

$$l = \frac{2K^2(K^2+1)}{(t_c-1)} \int_{-\infty}^1 \frac{dt}{(t^2+K^2)^2} \left[2t_c - t(1+t_c) + 2t_c^{1/2} [(1-t)(t_c-t)]^{1/2} \right] \quad (5.23)$$

The lift and drag coefficients are given by

$$C_L = \frac{8}{\ell} \frac{t_c^{1/2}}{t_c-1} K^2 (K^2+1) (I_1 - I_2) \cos \alpha \quad (5.24)$$

$$C_D = C_L \tan \alpha \quad (5.25)$$

where

$$\begin{aligned} I_2 &= \int_{t_c}^{\infty} \frac{[(t-1)(t-t_c)]^{1/2}}{(t^2+K^2)^2} dt \\ &= \frac{1}{2K^2} + \frac{1}{4K^3 (t_c^2+K^2)^{1/2} (u_1^2+v_1^2)} \cdot \\ &\quad \left\{ \frac{1}{2} \log \left(\frac{[q_1-u_1]^2+v_1^2}{[q_1+u_1]^2+v_1^2} \right) \left[t_c u_1 K (t_c-1) \right. \right. \\ &\quad \left. \left. - v_1 (2t_c^2 + K^2 t_c + K^2) \right] \right. \\ &\quad \left. - \arctan \left(\frac{2v_1 q_1}{q_1^2 - u_1^2 - v_1^2} \right) \cdot \right. \\ &\quad \left. \left[t_c v_1 K (t_c-1) + u_1 (2t_c^2 + K^2 t_c + K^2) \right] \right\} \\ I_1 &= \int_{-1}^{\infty} \frac{[(t+1)(t+t_c)]^{1/2}}{(t^2+K^2)^2} dt = I_2 + \frac{4\pi (t_c-1)^2}{(t_c^2+K^2)^2} \\ &\quad \cdot \frac{\xi}{u_1^2+v_1^2} \left[v_1 t_c K (t_c-1) + u_1 (2t_c^2 + K^2 t_c + K^2) \right] \end{aligned} \quad (5.26)$$

$$\left. \begin{aligned} q_1 &= (t_c^2 + K^2)^{1/2} \\ \xi &= \frac{q_1^3}{16K^3 (t_c-1)^2} \\ u_1 &= \left[\frac{K^2 + t_c}{2} + \frac{1}{2} \{ (K^2+1)(K^2+t_c^2) \}^{1/2} \right]^{1/2} \\ v_1 &= \frac{K(t_c-1)}{2u_1} \end{aligned} \right\} \quad (5.27)$$

The cavity length normalized with respect to the length of the plate is given approximately by:

$$L_c \cong \phi_c - \phi_a = \frac{t_c^2 - 1}{k^2 + t_c^2} \quad (5.28)$$

For streamlines we have

$$Z - z_A = \int_{t_A}^t e^{-\omega(t)} \frac{d\omega}{dt} dt$$

Using (5.19) the parametric representation of free streamlines is given by:

$$x(t) = x_A + \frac{2k^2(k^2+1)}{(t_c-1)} \int_1^t \frac{[\eta(t_c+1) - 2t_c] d\eta}{(\eta^2+k^2)^2}$$

$$y(t) = y_A + \frac{2k^2(k^2+1)}{(t_c-1)} \int_1^t \frac{[2t_c^{1/2} \{(\eta-1)(t_c-\eta)\}^{1/2} d\eta]}{(\eta^2+k^2)^2}$$

RESULTS AND DISCUSSION

The numerical results for the fully cavitating flow are shown in Figs. 25 and 26 for the lift and drag coefficients respectively. Experimental data from Parkin, Silberman, and Dawson, as reported by Wu [44], are also included.

It is seen that our results are in excellent agreement with Wu's results [44] for the fully cavitating regime, and consequently slightly higher than Larock and Street's data [18] in the range $0.1 < \sigma < 0.5$. The present theory slightly overpredicts the experimental data for small cavitation numbers but the overall agreement may be considered as satisfactory.

In Fig. 27 the results for the normalized cavity length vs. cavitation number for different angles of attack are given, including both partially and fully cavitating flow. The horizontal line in the graph marks the transition between fully cavitating regime (above) and partially cavitating regime (below).

In Figs. 28 and 29 the lift and drag coefficients for partially cavitating flow are reported for few values of angle of attack, and compared with Wu's [44] results. The results for the fully cavitating case are also included.

It is to be noted that our results for partially cavitating flow are different from Wu's for a certain range of values of σ . In particular, the drag coefficient in the present theory is always positive

and increasing with increasing σ , while in Wu's theory [44] it is decreasing in the partially cavitating range and eventually becomes negative, which is physically unrealistic.

In the limit for large σ our model does not yield the fully wetted limit and also it does not predict a lift maximum [17]. However, it is interesting to note that our results do tend to the correct fully cavitating limit and values in the transition range are obtained, which were intuitively interpolated by Wu [44].

CONCLUDING REMARKS

Linearized theories for partially cavitating flow have been introduced by Acosta [1] and Geurst [15]. Camber effects of a partially cavitating hydrofoil have been investigated by Geurst and Verbrugh [16]. Experimental results for hydrofoils of a few different plan forms are given by Meijer [25].

The common feature of the linearized theories is that they break down for cavity lengths close to unity [43], as they predict a singular behaviour of the flow in the transition region, when the rear end of the cavity approaches the trailing edge.

In the present theory the behaviour of the flow in the transition region is smooth and non-singular, but as already mentioned, the fully wetted limit is not achieved. In actual cavity flows, when the cavitation number σ increases beyond a certain critical value, the

cavity collapses and disappears and the lift coefficient levels off to the fully wetted value after reaching a maximum. It appears that the present theory does not indicate the cavity collapse and is thus restricted to the range of cavitation numbers below the critical value, where the lift achieves a maximum.

The experimental results of Meijer [25] indicate an instability of the cavity flow in the transition region, which would seem to support the results of linearized theories. In view of these results and the scarcity of available data, it seems that further experimental investigation is needed in order to obtain more detailed information on the behaviour of the flow in the partially cavitating range, especially when the length of the cavity is nearly equal to that of the plate.

Table 1
 Comparison of Riabouchinsky, Re-entrant Jet and Single Spiral Vortex Models;
 Cavity Length, Cavitation Number and Drag

Wedge half angle	Cavitation number	Riabouchinsky Model		Re-entrant Jet Model		Single Spiral Vortex Model	
		Cavity length	Drag Coefficient	Cavity length	Drag Coefficient	Cavity length	Drag Coefficient
$\pi/2$	0.05	6930	.93	6770	.92	6730	.925
	0.10	1760	.97	1790	.97	1760	.968
	0.10	482	1.1	495	1.1	482	1.2
	0.42	97	1.3	103	1.3	98	1.4
	2.0	13	2.7	16	2.7	14	2.8
$\frac{\pi}{3}$	0.05	2990	.79	3004	.78	2985	.78
	0.1	785	.82	792	.82	783	.82
	1.0	14	1.7	15	1.6	14	1.6
$\frac{\pi}{4}$	0.05	1685	.7	1692	.7	1685	.7
	0.10	441	.71	446	.71	442	.71
	1.42	6	1.7	7	1.7	6	1.6

APPENDIX A

In this appendix we shall discuss the general solution of the Riemann-Hilbert mixed boundary value problem in an upper half plane [36].

It is assumed that the function $\omega(t)$ is regular in the upper half plane and satisfies given boundary conditions on the real axis. The function may have isolated singularities (it can not have essential singularities as mentioned by Birkhoff and Zarantonello [4]) on the boundary, provided Holder's inequality is satisfied at the singularities. By a Hölder condition of index λ we mean that $|\phi(z) - \phi(z_0)| < M|z - z_0|^\lambda$ for some constants M and λ .

Let $H(t)$ be the homogeneous solution of the R-H mixed boundary value problem. In construction of the homogeneous solution, given boundary values are put equal to zero. Now, the imaginary part of the new function $Q(t) = \frac{\omega(t)}{H(t)}$ is known along the real axis. And the general solution of the reduced boundary value problem is [6]

$$\omega(t) = \frac{H(t)}{\pi} \int_{-\infty}^{\infty} \frac{f_m\left\{\frac{\omega(\eta)}{H(\eta)}\right\}}{\eta - t} d\eta + \sum_{j=0}^{\infty} A_j t^j \quad (\text{A.1})$$

The result does not depend on the choice of the branch of $H(t)$; however, it is important to remain on the same branch on the upper border of the real axis.

Consider the most general homogeneous solution

$$H(t) = i \frac{p(t)}{q(t)} \prod (t - b_j)^{\pm 1/2} \quad (\text{A.2})$$

where $p(t)$ and $q(t)$ are the polynomials of arbitrary order and b_j are real. Since zeros of $q(t)$ are poles of $H(t)$ and hence of $\omega(t)$, the polynomial $q(t)$ must be constant or of zero order. If $\omega(t)$ has a pole in the upper half-plane it means the function is not regular, and if $\omega(t)$ has a pole on the boundary, the Hölder's condition is violated.

The polynomial $p(t)$ may have any number of real roots, or an even number of complex roots.

Case 1.

When $p(t)$ has a real root $t = \alpha$, then we may write

$$H(t) = (t - \alpha) h(t) \quad (\text{A.3})$$

Substituting in Eq. (A.1) we have

$$\omega(t) = \frac{(t - \alpha) h(t)}{\pi} \left\{ \int_{-\infty}^{\infty} \frac{\omega_0 d\eta}{(\eta - \alpha)(\eta - t) R(\eta)} + \sum_{j=0}^{\infty} A_j t^j \right\} \quad (\text{A.4})$$

where ω_0 is known from the boundary conditions.

Since

$$\frac{1}{(\eta - t)(\eta - \alpha)} = \frac{1}{(t - \alpha)(\eta - t)} - \frac{1}{(t - \alpha)(\eta - \alpha)}$$

Eq. (A.4) reduces to

$$\omega(t) = \frac{h(t)}{\pi} \left\{ \int_{-\infty}^{\infty} \frac{\omega_0 d\eta}{(\eta - t) R(\eta)} - \int_{-\infty}^{\infty} \frac{\omega_0 d\eta}{(\eta - \alpha) R(\eta)} + (t - \alpha) \sum A_j t^j \right\}$$

Since $\int_{-\infty}^{\infty} \frac{\omega_0 d\eta}{(\eta - \alpha) R(\eta)}$ is not a function of t we have:

$$\omega(t) = \frac{h(t)}{\pi} \left\{ \int_{-\infty}^{\infty} \frac{\omega_0 d\eta}{(\eta - t) R(\eta)} + \sum B_j t^j \right\} \quad (\text{A.5})$$

where

$$B_0 = \int_{-\infty}^{\infty} \frac{\omega_0 d\eta}{(\eta-a)h(\eta)}$$

This equation is identical to Eq. (A.1) except that $H(t)$ is replaced by $h(t)$. We can reduce the order of the polynomial $p(t)$, if it has no real roots, by the same argument.

Case II.

$p(t)$ has a set of even complex roots. In this case, the homogeneous solution may be written as

$$H(t) = (t^2+a^2)h(t)$$

and the solution $\omega(t)$ takes the following form:

$$\omega(t) = \frac{(t^2+a^2)h(t)}{\pi} \left\{ \int_{-\infty}^{\infty} \frac{\omega_0 d\eta}{(\eta-t)(\eta^2+a^2)h(\eta)} + \sum A_j t^j \right\}. \quad (\text{A.6})$$

Again, by the method of partial fractions it can be reduced to (A.1).

Lastly, we shall consider the double sign (\pm) occurring in Eq. (A.2). If we take negative sign, we may write

$$H(t) = \frac{h(t)}{(t-b)^{1/2}}$$

and the solution for $\omega(t)$ is

$$\omega(t) = \frac{h(t)}{\pi(t-b)^{1/2}} \left\{ \int_{-\infty}^{\infty} \frac{\omega_0 (\eta-b)^{1/2}}{(\eta-t)h(\eta)} d\eta + \sum A_j t^j \right\} \quad (\text{A.7})$$

Since all A_j 's are arbitrary constants, we may write

$$\sum A_j t^j = - \int_{-\infty}^{\infty} \frac{\omega_0 d\eta}{(\eta-b)^{1/2} h(\eta)} + (t-b) \sum B_j t^j \quad (\text{A.8})$$

Substituting Eq. (A.8) into Eq. (A.7) we have

$$\omega(t) = \frac{(t-b)^{1/2} h(t)}{\pi} \left\{ \int_{-\infty}^{\infty} \frac{\omega_0 d\eta}{(\eta-t)(\eta-b)^{1/2} R(\eta)} + \sum B_j t^j \right\} \quad (\text{A.9})$$

Hence, we conclude that the choice of sign is immaterial. This completes the proof of the general solution of the Riemann-Hilbert problem.

APPENDIX B

This appendix is based on the results already discussed by Cheng and Rott [6] and Song [35].

In this appendix we shall prove the existence and uniqueness of the function $w(z) = u(x,y) - iv(x,y)$, $z = x + iy$, which is analytic on the upper half of the z -plane, finite at infinity, sectionally continuous on the real axis except at the origin and satisfying the following boundary conditions on the real axis:

$$\begin{array}{ll}
 x \leq a_1 & v = v_1(x) \\
 a_1 \leq x \leq a_2 & u = u_2(x) \\
 a_2 \leq x \leq a_3 & v = v_3(x) \\
 \dots & \dots \\
 a_n \leq x & \left\{ \begin{array}{l} v = v_{n+1}(x) \text{ if } n \text{ is even} \\ u = u_{n+1}(x) \text{ if } n \text{ is odd} \end{array} \right.
 \end{array}$$

where $v_1(x), u_2(x), \dots$ etc. are sectionally continuous, i.e., bounded

in every closed interval, finite at infinity, and $a_1 < a_2 < a_3 \dots < a_n$.

When n is odd ($n = 2m+1$ $m = 0, 1, 2, \dots$), the solution of the above problem is well known and is given by

$$\omega(z) = -\frac{H(z)}{\pi} \int_{-\infty}^{\infty} \frac{q(\tau) d\tau}{\tau - z} \quad (\text{B.1})$$

The function (B.1) is the unique solution

$$if \int_{-\infty}^{\infty} q(\tau) d\tau = \int_{-\infty}^{\infty} \tau q(\tau) d\tau = \dots = \int_{-\infty}^{\infty} \tau^{m-1} q(\tau) d\tau = 0 \quad (\text{B.2})$$

where

$$H(z) = [(z-a_1)(z-a_2)\dots(z-a_{n-1})(a_n-z)]^{1/2} \quad (\text{B.3})$$

$$\left. \begin{aligned} q(\tau) &= \frac{v_i(\tau)}{H(\tau)} & if \ i \text{ is odd} \\ q(\tau) &= i \frac{u_i(\tau)}{H(\tau)} & if \ i \text{ is even} \end{aligned} \right\} \quad (\text{B.4})$$

It is important to remain on the same branch on the upper border of the real axis both for $H(z)$ in (B.1) and $H(\tau)$ in (B.4).

The result does not depend on the choice of branch. Since the integral (B.1) has a singularity at $\tau = z$ we must consider the principal value there.

Proof: To show the existence, the first thing to note is that the function (B.1) is analytic on the upper half of the z -plane, sectionally continuous on the real axis except at the origin, and satisfies the given boundary conditions. Therefore, we shall only show that the function is finite at infinity. For large z , the function $\frac{H(z)}{z-\tau}$ behaves like $z^{m-1} + z^{m-2}\tau + \dots + z\tau^{m-2} + \tau^{m-1} + \dots$ therefore the function (B.1) behaves like

$$\frac{z}{\pi} \int_{-\infty}^{\infty} q(\tau) d\tau + \frac{z^{m-2}}{\pi} \int_{-\infty}^{\infty} \tau q(\tau) d\tau + \dots + \frac{1}{\pi} \int_{-\infty}^{\infty} \tau^{m-1} q(\tau) d\tau + o\left(\frac{1}{z}\right) \quad (\text{B.5})$$

From the condition (B.2) it is obvious that the function is finite at infinity. Therefore (B.1) is a solution.

To prove uniqueness let us assume that there is another solution $w_1(z)$, then

$$W(z) = w(z) - w_1(z) \quad (\text{B.6})$$

is also a solution of the problem. This function is analytic on the upper half of z -plane, finite at infinity, sectionally continuous on the real axis except at the origin and satisfying the following boundary conditions on the real axis:

$$\left. \begin{array}{l} x \leq a_1 \\ a_1 \leq x \leq a_2 \\ \dots \\ a_n \leq x \end{array} \right\} \begin{array}{l} v = 0 \\ u = 0 \\ \dots \\ v = 0 \end{array} \quad (\text{B.7})$$

Therefore, we can express the function

$$W(z) = AH(z) \quad (\text{B.8})$$

where A is constant. Since $H(z)$ is not finite at infinity the constant A must be zero. This means $W(z) = 0$ and

$$w_1(z) = w(z)$$

and the solution is unique.

The result can be proven in a similar manner when n is even.

BIBLIOGRAPHY

- [1] Acosta, A.J., 'A Note on Partial Cavitation of Flat Plate Hydrofoils' Hydrodynamics Lab., Cal. Tech., Pasadena, California, Report No. E-19-9, October 1955.
- [2] Acosta, A.J., 'The Effects of a Longitudinal Gravitational Field on the Supercavitating Flow over a Wedge', Journal of Applied Mechanics, 28, Trans. ASME, 83, Series E, pp. 188-192, 1961.
- [3] Ai, D.K., 'The Wall Effects in Cavity Flows', Trans. ASME, Journal of Basic Engineering, Vol. 88, 1, pp. 132-138, March 1966.
- [4] Arnoff, E.L., 'Re-entrant Jet Theory and Cavity Drag for Symmetric Wedges', Navord Report 1298, No. TS 368, China Lake, 1959.
- [5] Birkhoff, G. and Zarantonello, E.H., 'Jets, Wakes and Cavities', Academic Press, 1957.
- [6] Cheng, H.K. and Rott, N., 'Generalization of the Inversion Formula of Thin Airfoil Theory', Journal of Rational Mechanics and Analysis, 3, pp. 357-382, 1954.
- [7] Churchill, R.V., 'Complex Variables and Applications', 2nd Ed. McGraw-Hill, New York, 1960.
- [8] Cohen, H., Sutherland C.D. and Yih- QTU , 'The Wall Effects in Cavitating Hydrofoil Flow', Journal of Ship Research, November 1957, pp. 31-39.
- [9] Eisenberg, P., 'On the Mechanism and Prevention of Cavitation' David Taylor Model Basin Rep. 712, 1950.
- [10] Eisenberg, P., and Tulin, M.P., 'Cavitation', Section 12, Handbook of Fluid Dynamics, (Editor Streeter,) McGraw-Hill 1961.
- [11] Fabula, A., 'Thin Airfoil Theory Applied to Hydrofoils with Single Finite Cavity and Arbitrary Free Streamline Detachment', Journal of Fluid Mechanics, 12, 2, pp. 227-248, 1962
- [12] Gilbarg, D., 'Jets and Cavities', Handbuch der Physik, Vol. 9, Springer-Verlag, Berlin, Germany, pp. 311-445, 1960.

- [13] Gilbarg, D. and Serrin, J., 'Free Boundaries and Jets in the Theory of Cavitation', *Journal of Mathematics and Physics*, 29 pp. 1-12, 1950.
- [14] Geurst, J.A., 'Linearized Theory of Two-Dimensional Cavity Flows', Thesis, Delft Tech. Inst., Netherlands, 1961.
- [15] Geurst, J.A., 'Linearized Theory for Partially Cavitated Hydrofoils', *Int. Shipbuilding Progress*, Vol. 6, No. 60, pp. 369-384, August 1959.
- [16] Geurst, J.A. and Verbrugh, P.J., 'A Note on Camber Effects of a Partially Cavitated Hydrofoil', *Int. Shipbuilding Progress*, Vol. 6, 61, pp. 409-414, September 1959.
- [17] Lamb, H., 'Hydrodynamics', 6th Edition, Dover Publications, New York, 1945, pp. 96-105.
- [18] Larock, B.E. and Street, R.L., 'A Riemann-Hilbert Problem for Non-Linear Fully Cavitating Flow', *Journal of Ship Research*, 9, 3, pp. 170-178, 1965.
- [19] Larock, B.E. and Street, R.L., 'A Non-Linear Solution for a Fully Cavitating Hydrofoil Beneath a Free Surface', *Journal of Ship Research*, 11, 2, pp. 131-140, 1967.
- [20] Larock, B.E. and Street, R.L., 'Cambered Bodies in Cavitating Flow- A Non-Linear Analysis and Designing Procedure', *Journal of Ship Research*, 12, 1, pp. 1-13, 1968.
- [21] Larock, B.E. and Street, R.L., 'A Non-Linear Theory for Fully Cavitating Hydrofoil in a Transverse Gravity Field', *Journal of Fluid Mechanics*, 29, 2, pp. 317-336, 1967.
- [22] Lavrent'ev, M.A., 'Variational Methods for Boundary Value Problems for System of Elliptic Equations', (Translated by J.R.M. Radok), P. Noordhoff Ltd., Groningen, 1963, Netherlands, pp. 45-48.
- [23] Lenau, C.W. and Street, R.L., 'A Non-Linear Theory for Symmetric, Supercavitating Flow in a Gravity Field', *Journal of Fluid Mechanics*, 21, 2, pp. 257-280, 1965.
- [24] Lighthill, M.J., 'A Note on Cusped Cavities', Aeronautics Research Council, Report and Memo 2328, 1945.
- [25] Meijer, M.C., 'Some Experiments on Partially Cavitating Hydrofoils', *Int. Shipbuilding Progress*, Vol. 6, 60, pp. 361-368, August 1959.

- [26] Mikhlin, S.G., 'Integral Equations', Translation by A.H. Armstrong, Macmillan Co., 1964.
- [27] Milne-Thomson, L.M., 'Theoretical Hydrodynamics', Macmillan Co., 4th Edition, pp. 283-284, 1962.
- [28] Parkin, B.R., 'A Note on the Cavity Flow Past a Hydrofoil in a Liquid with Gravity', Report No. 47-9, Engineering Division, California Tech., Pasadena, 1957.
- [29] Parkin, B.R., 'Linearized Theory of Cavity Flow in Two-Dimensions' Rand Corp. Report No. P1745, Santa Monica, California, 1959.
- [30] Plesset, M. and Shaffer, P., 'Cavity Drag in Two and Three Dimensions', Journal of Applied Physics, 19, pp. 934-937, 1948.
- [31] Poole, E.G.C., 'On the Discontinuous Motion Produced in an Infinite Stream by Two Plane Obstacles', 'Proc. Lond. Math. Soc.', pp. 425-452, 1923.
- [32] Pykhtev, G.N., Private Communication.
- [33] Riabouchinsky, D., 'On Steady Fluid Motion with Free Surface', Proc. Lond. Math. Soc., 19, pp. 206-215, 1920.
- [34] Roshko, A., 'A New Hodograph for Free Streamline Theory', NACA TN 3168, 1954.
- [35] Song, C.S., 'A Note on the Linear Theory of Two-Dimensional Separated Flows About Thin Bodies', St. Anthony Falls Hydraulic Lab., Tech. Paper No. 39, Series B, 1962.
- [36] Song, C.S., 'A Quasi-linear and Linear Theory for Non-Separated and Separated Two-Dimensional, Incompressible Irrotational Flow About-Lifting Bodies', St. Anthony Falls Lab., T. No. 63, Series B, 1963.
- [37] Street, R.L., 'Supercavitating Flow about a Slender Wedge in a Transverse Gravity Field', Journal of Ship Research, 7, 1, pp. 14-23, 1963.
- [38] Street, R.L., 'A Note on Gravity Effects in Supercavitating Flow', Journal of Ship Research, 8, 1, pp. 39-45, 1965.
- [39] Tulin, M.P., 'Steady Two-Dimensional Cavity Flows about Slender Bodies', David Taylor Model Basin Report, 834, 1953.
- [40] Tulin, M.P., 'Supercavitating Flows—Small Perturbation Theory', Journal of Ship Research, 7, 3, pp. 16-37, 1964.

- [41] Tulin, M.P., 'The Shape of Cavities in Supercavitating Flows', XI IUTAM Congress Paper, Munich, Germany, September 1964.
- [42] Wu, T.Y. 'A Free Streamline Theory for Two-Dimensional Fully Cavitated Hydrofoils' Journal of Mathematics and Physics, 35, pp. 236-265, 1956.
- [43] Wu, T.Y., 'A Note on the Linear and Non-linear Theories for Fully Cavitated Hydrofoils', Hydrodynamics Lab. Rept., No. 21-22, Cal. Tech., 1956.
- [44] Wu, T.Y., 'A Wake Model for Free-Streamline Theory - Part I', Journal of Fluid Mechanics, 13, 2, pp. 161-181, 1962.
- [45] Wu, T.Y., 'A Wake Model for Free-Streamline Theory - Part II', 18, 1, pp. 65-93, 1964.
- [46] Woods, L.C., 'The Theory of Subsonic Plane Flow' Cambridge University Press, 1961.
- [47] Wang, Chan^o -^v4, 'Local Instability of Hydrodynamic Cavities', MIT Fluid Dynamics Research Lab., Report No. 63-4, December 1964.

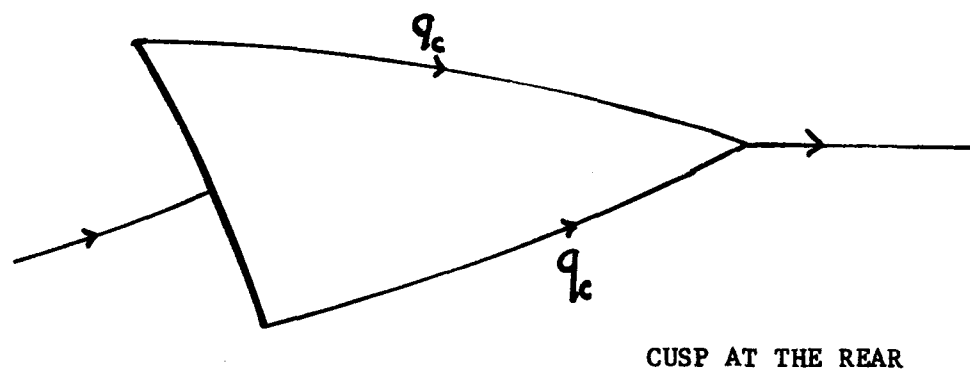
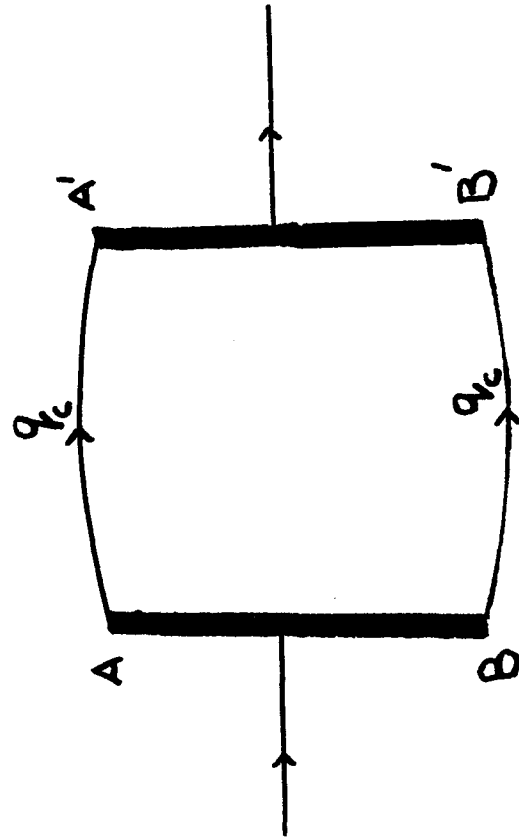


Fig. 1

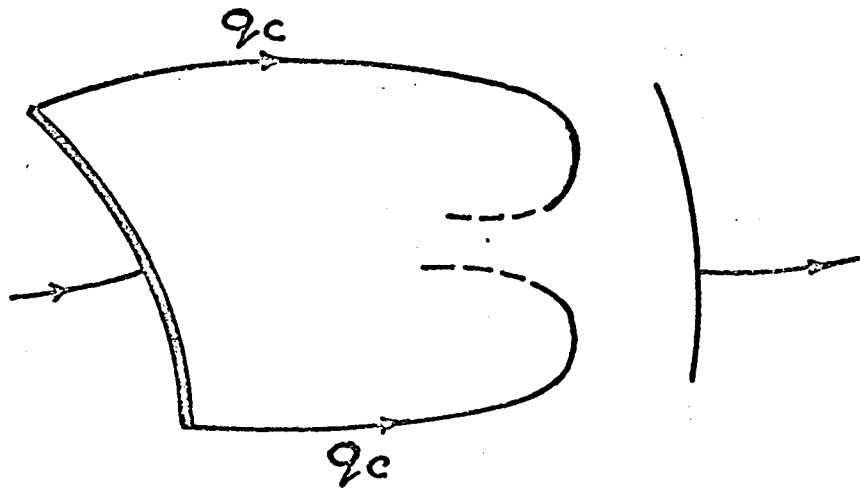
Physical flow plane represented by cusped cavity
model for fully cavitating flow.



(RIABOUCHINSKY MODEL 1920)

FIG. 2

Physical flow plane represented by Riabouchinsky's
model for fully cavitating flow



Re-entrant Jet Termination
[Efros-Kreisel-Gilbarg Model 1954.]

Fig. 3

Physical flow plane represented by re-entrant jet model
for fully cavitating flow

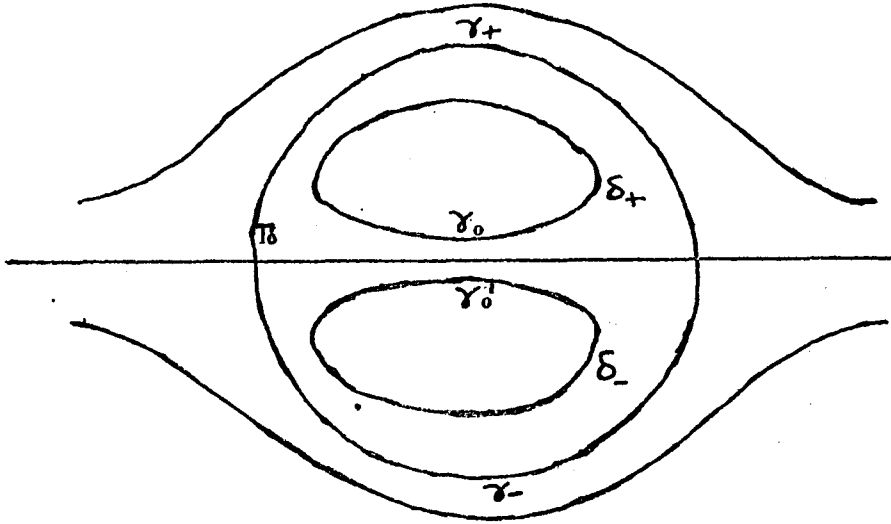


Fig. 4

Physical flow plane represented by Lavrent'ev model
for fully cavitating flow

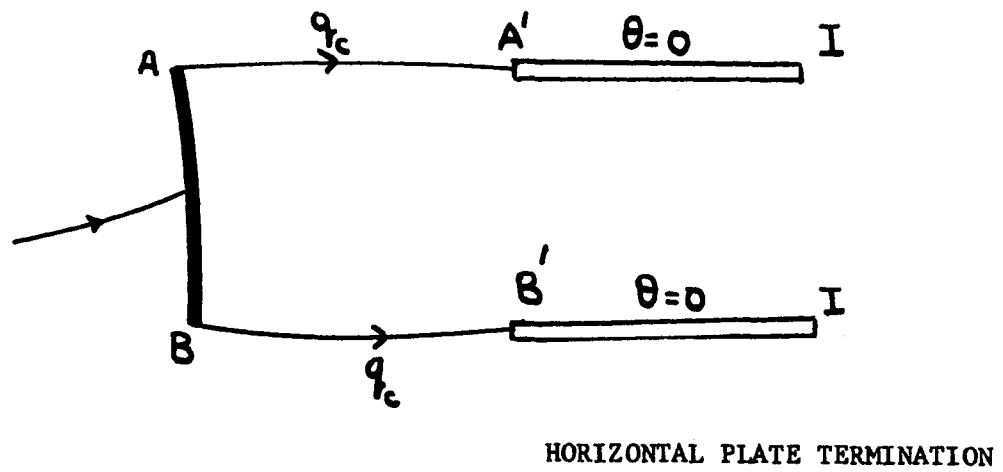


Fig. 5

Physical flow plane represented by Roshko's model for
fully cavitating flow.

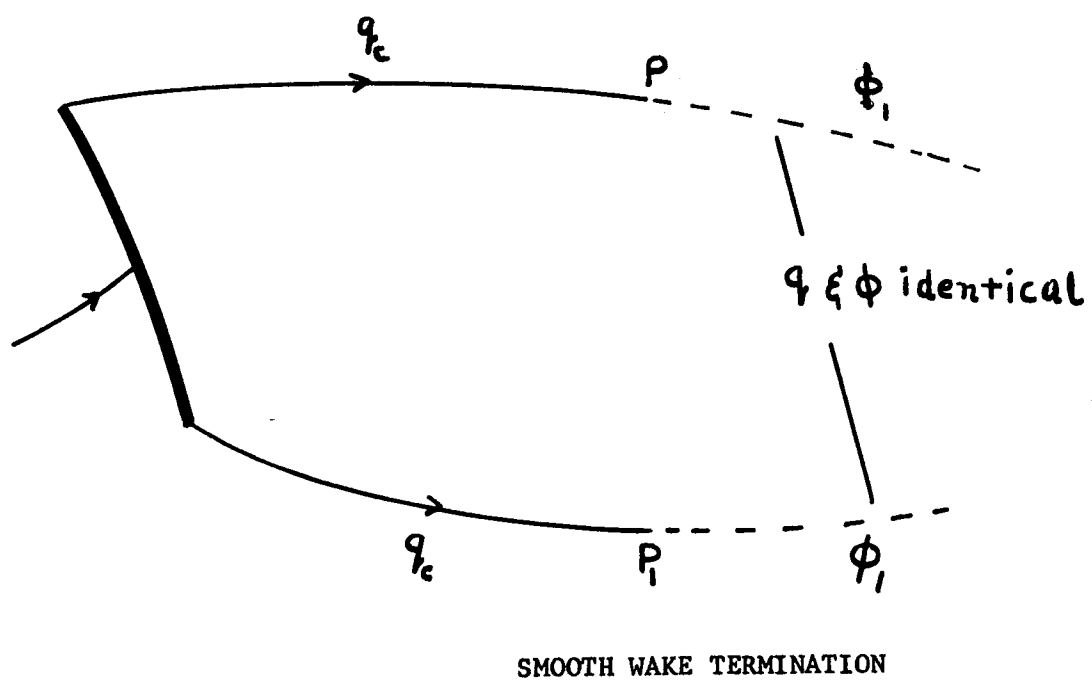


Fig. 6

Physical flow plane represented by wake model
for fully cavitating flow.

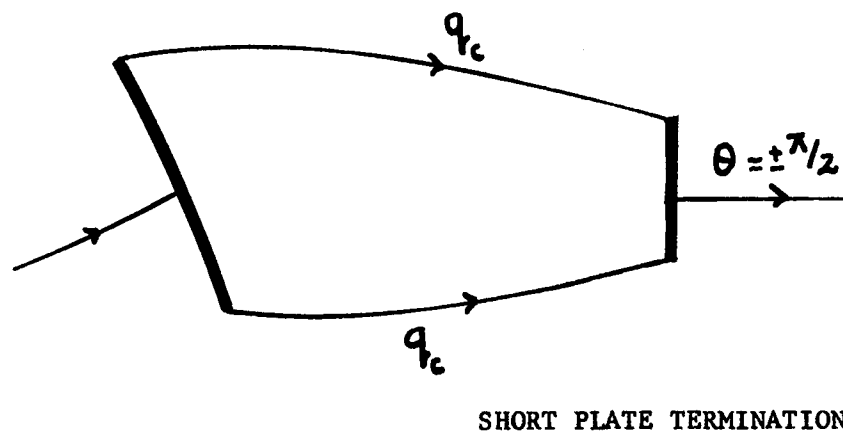
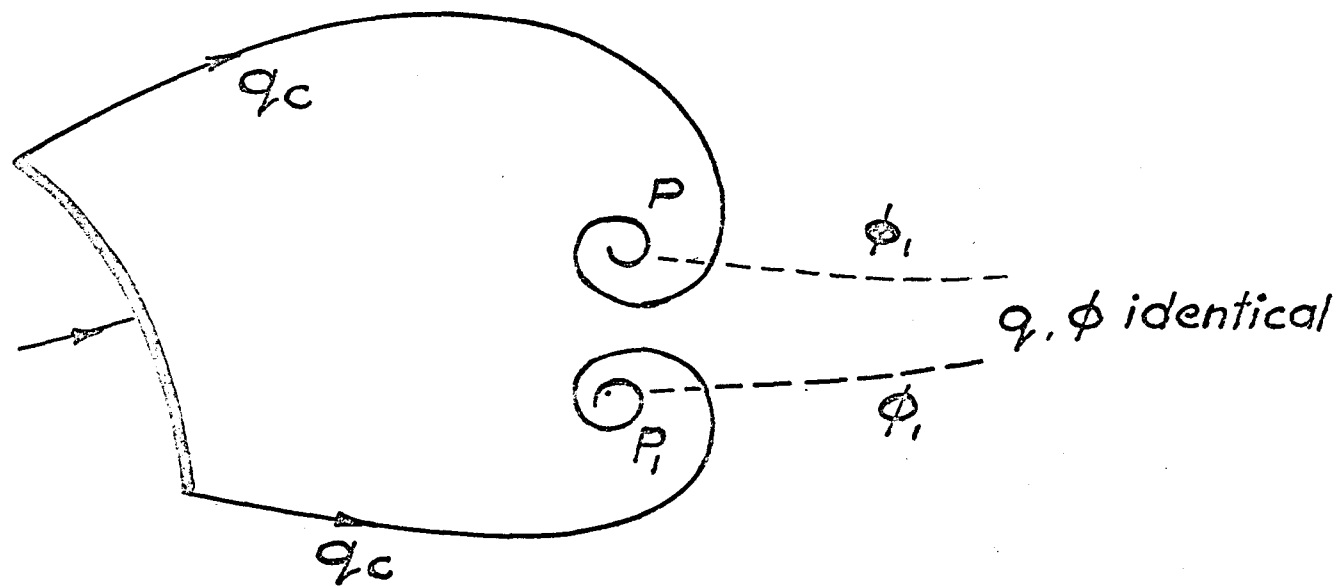


Fig. 7

Physical flow plane represented by modified
Riabouchinsky model.



*Single Spiral Vortex - Smooth Wake Termination
[Tulin's Single Spiral Vortex Model 1964]*

Fig. 8

Physical flow plane represented by single spiral vortex
model for fully cavitating flow

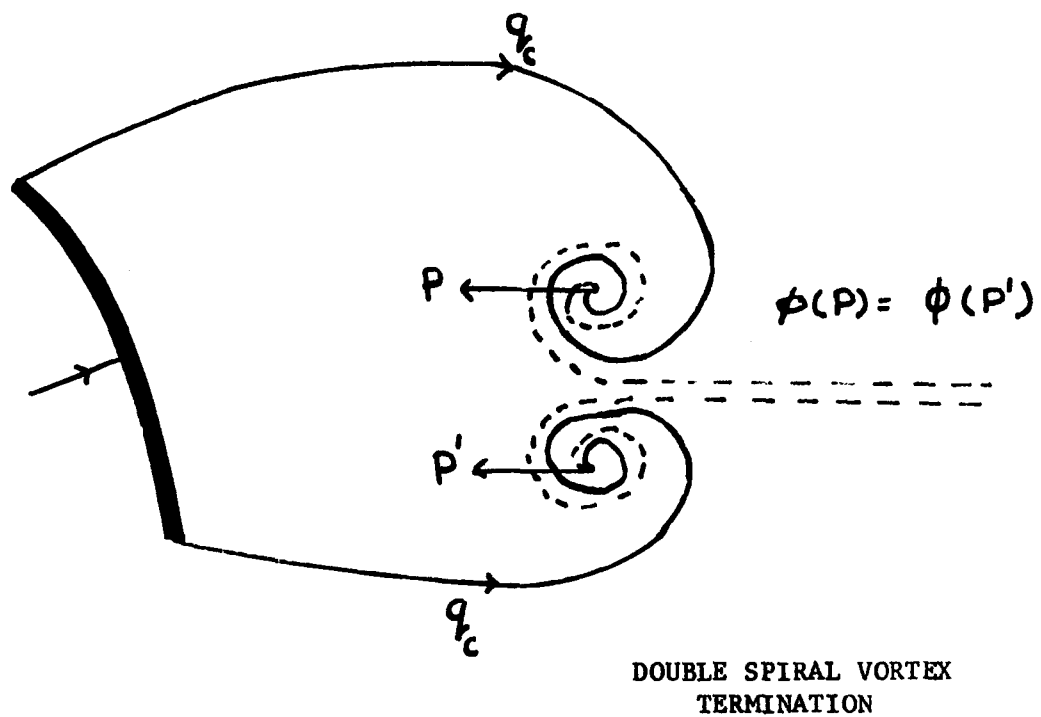


Fig. 9

Physical flow plane represented by double spiral vortex model
for fully cavitating flow.

Z-PLANE

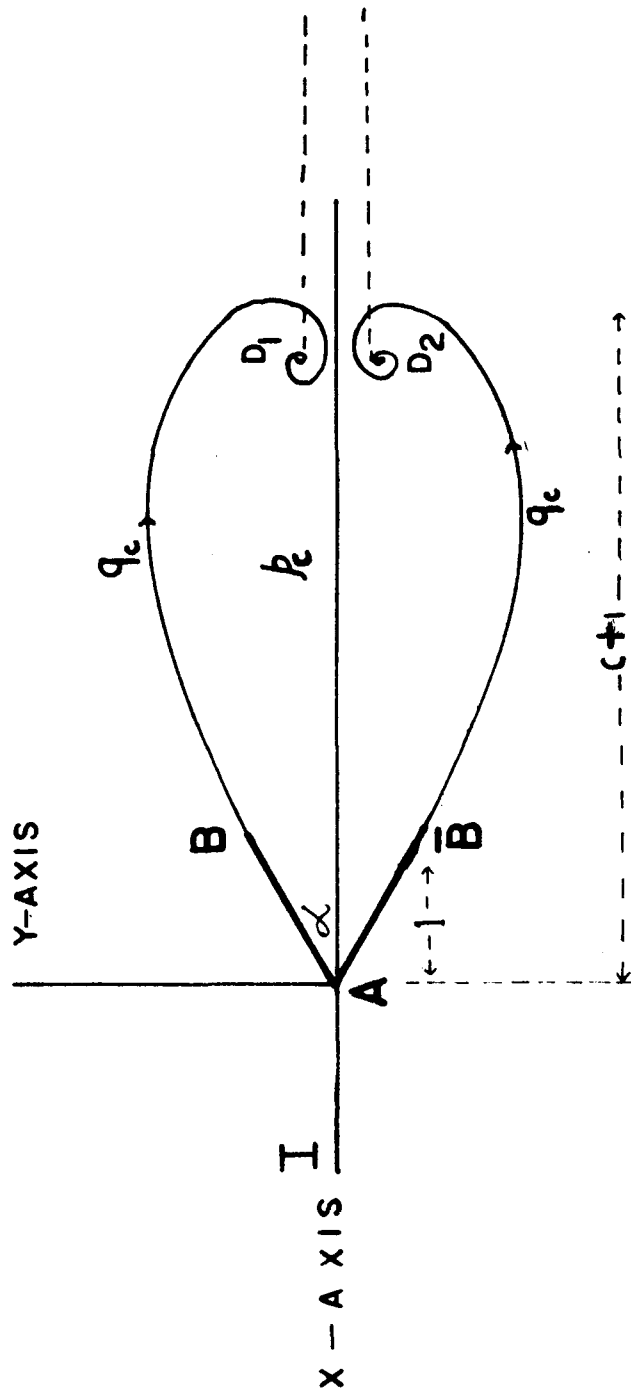


Fig. 10

Physical Flow plane for Fully Cavitating Flow
(wedge)

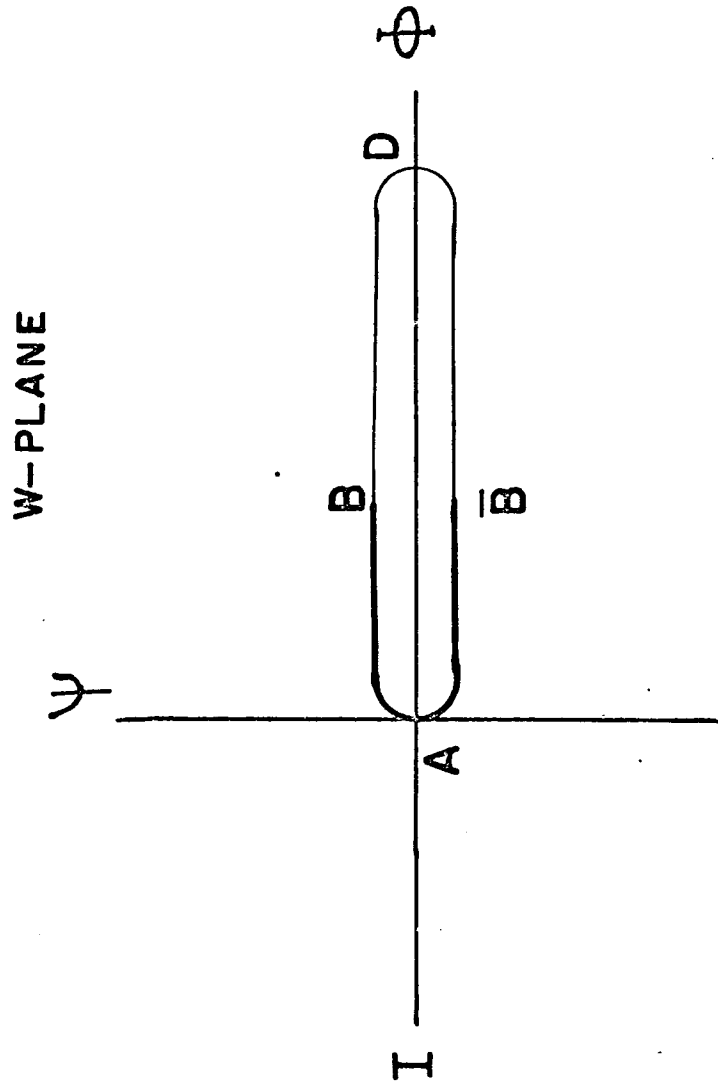


Fig. 11

Complex potential plane for fully cavitating
flow (wedge)

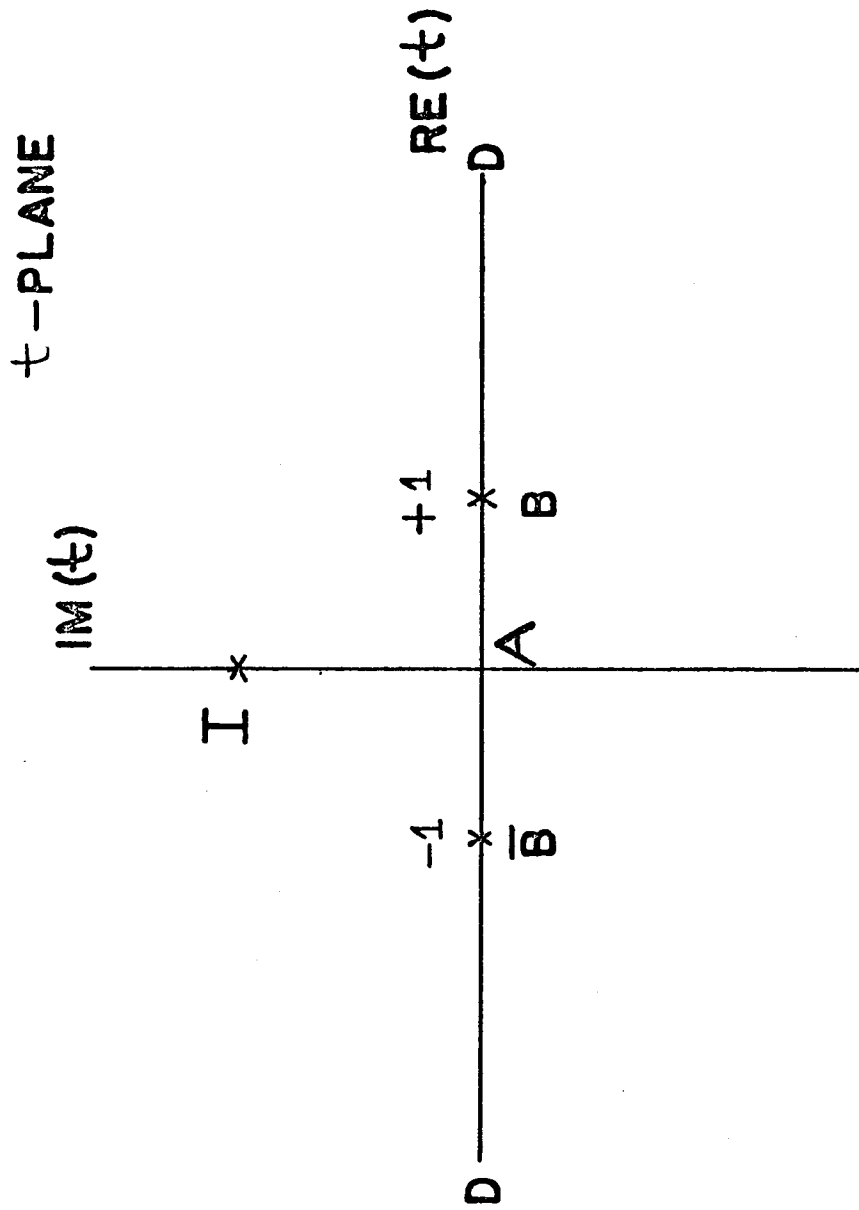


Fig. 12

Parametric plane for fully cavitating flow (wedge)

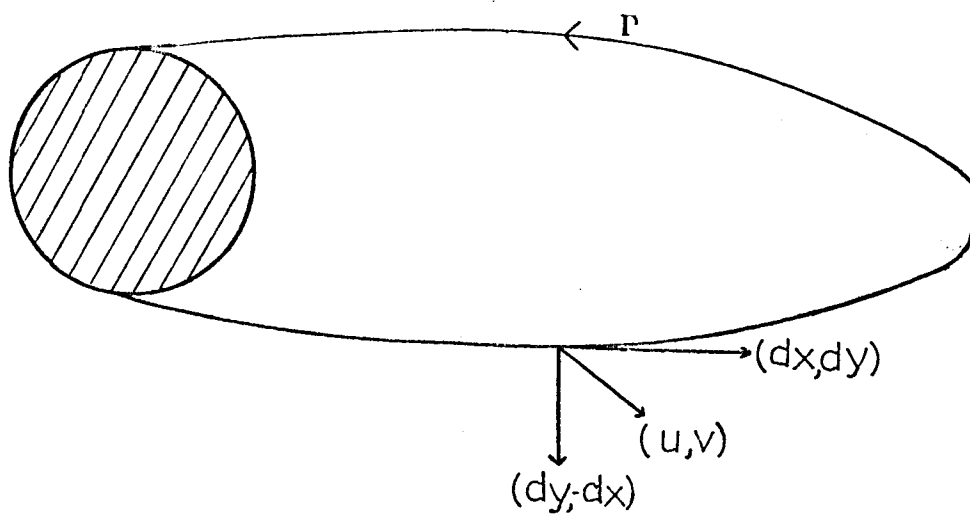


Fig. 13

Flow showing body-cavity system

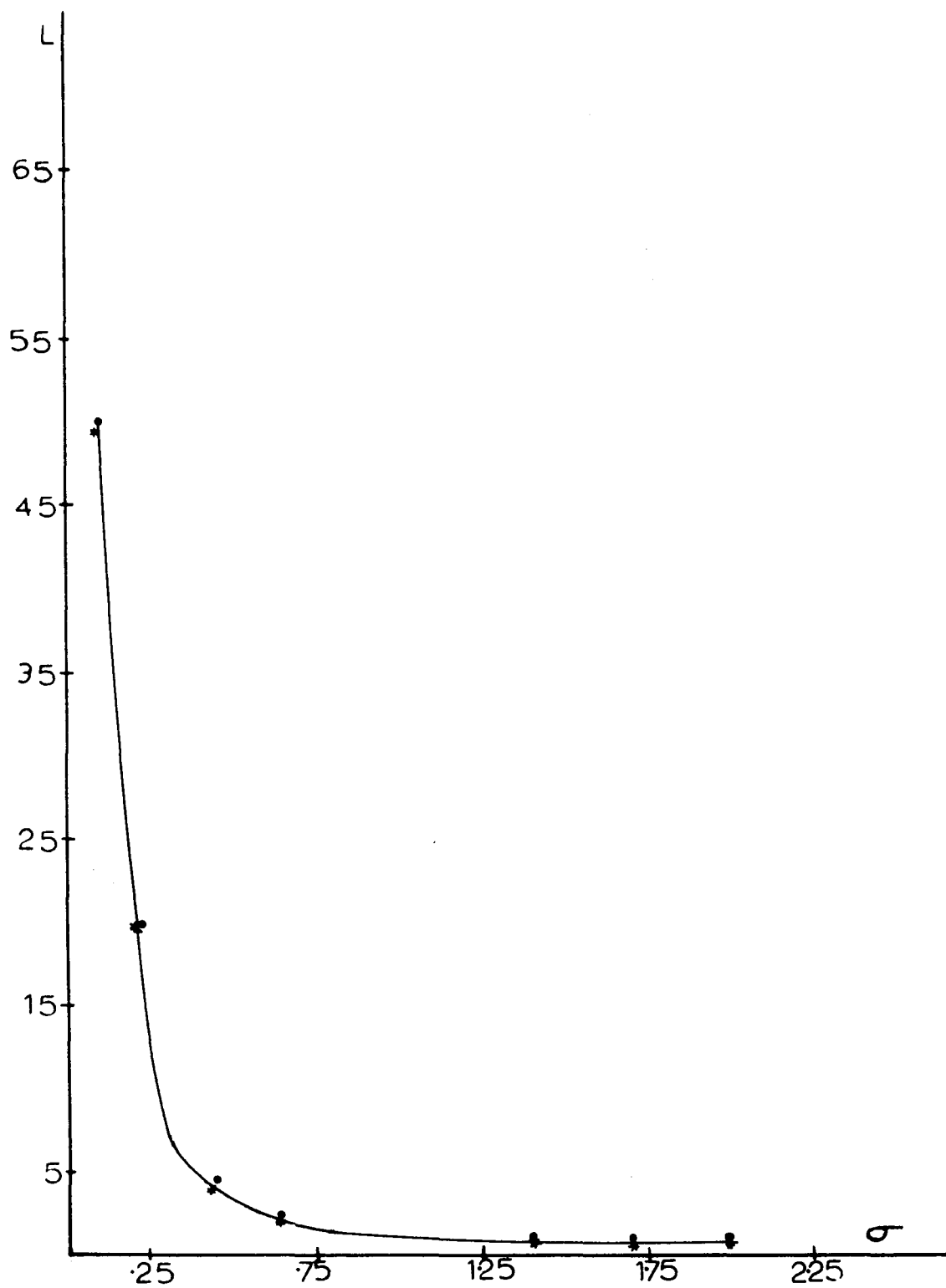


Fig. 14

Cavity length against cavitation number for single spiral vortex model for $\alpha = 15^\circ$ (wedge). Numerical results for Riabouchinsky model (*) and for re-entrant jet model (•) are also included.

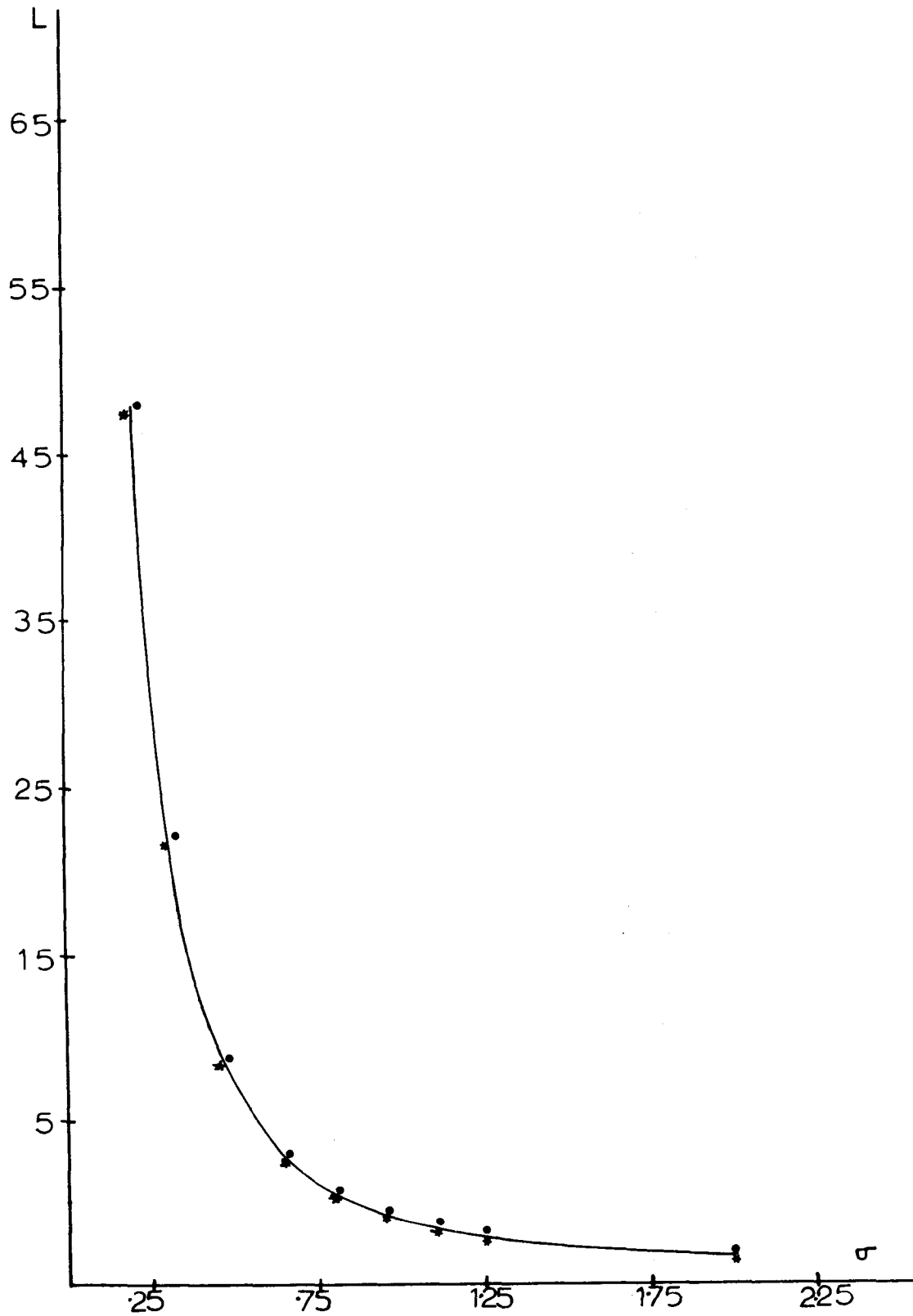


Fig. 15

Cavity length against cavitation number for single spiral vortex model for $\alpha = 30^\circ$. Numerical results for Riabouchinsky model (*) and re-entrant jet model (●) are also included

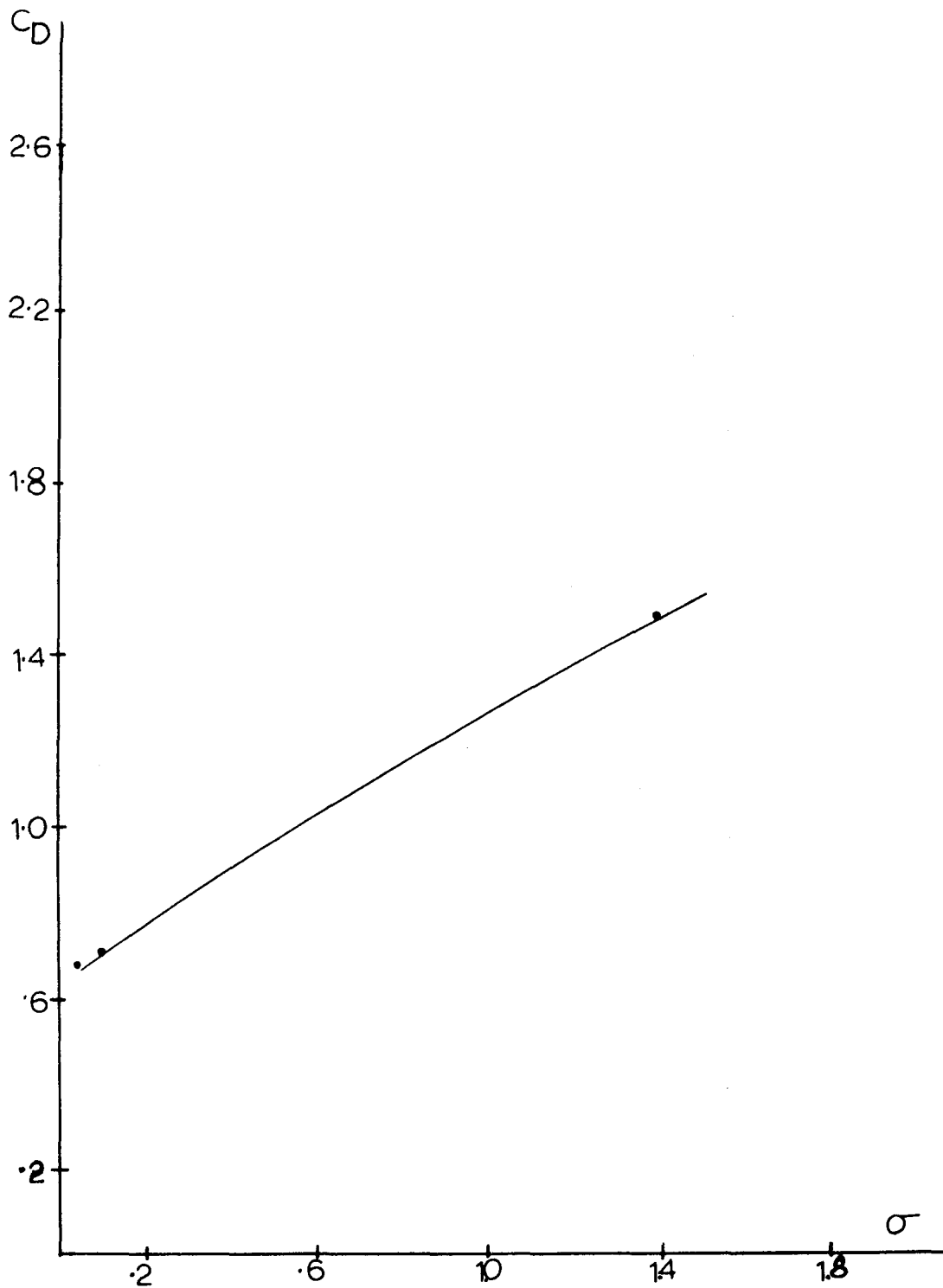


Fig. 16

Drag coefficient vs cavitation number for single spiral vortex model for $\alpha = 45^\circ$. The numerical results for re-entrant jet model (\bullet) are also included

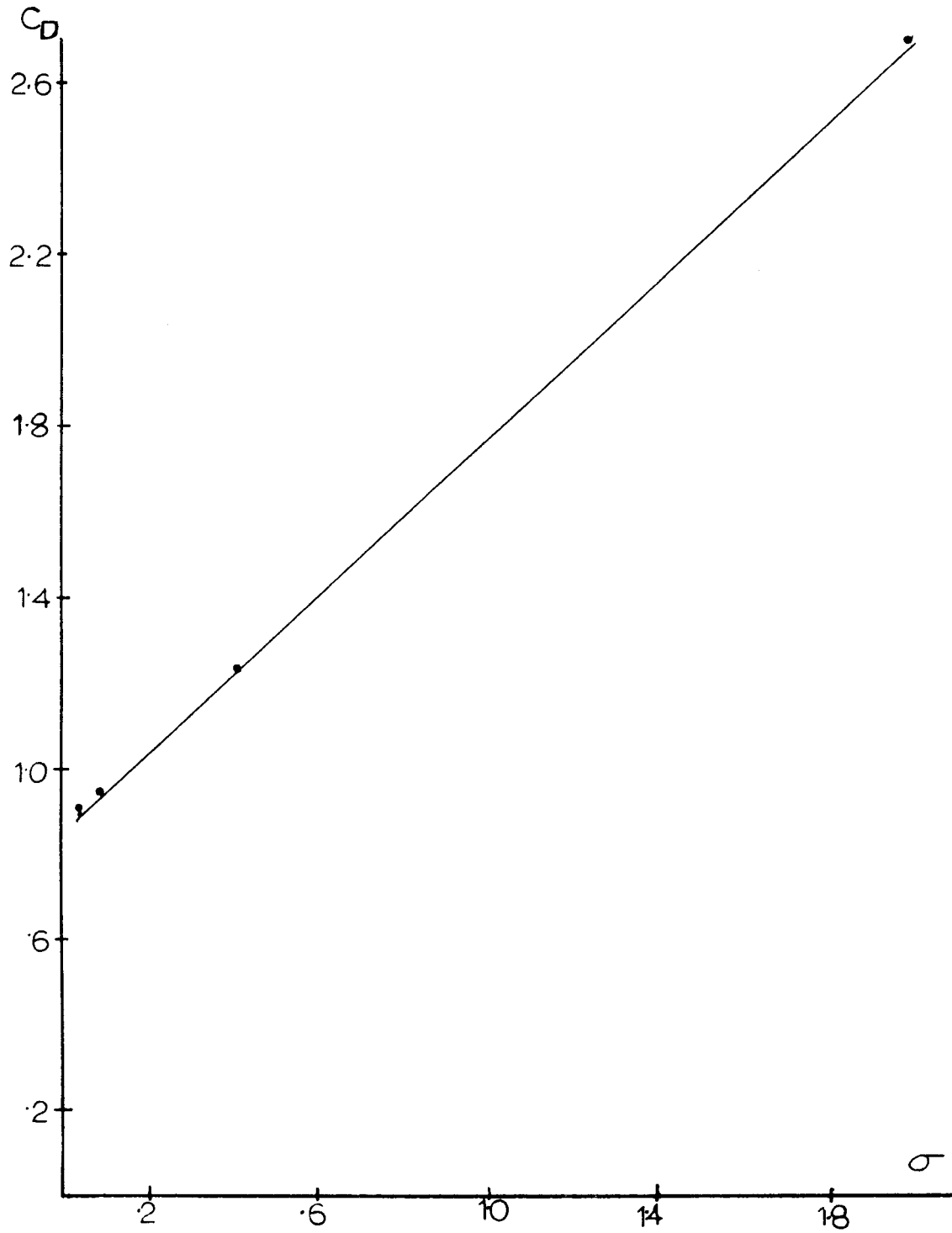


Fig. 17

Drag coefficient vs cavitation number for single spiral vortex model for $\alpha = 90^\circ$. The numerical results for re-entrant jet model (\bullet) are also included

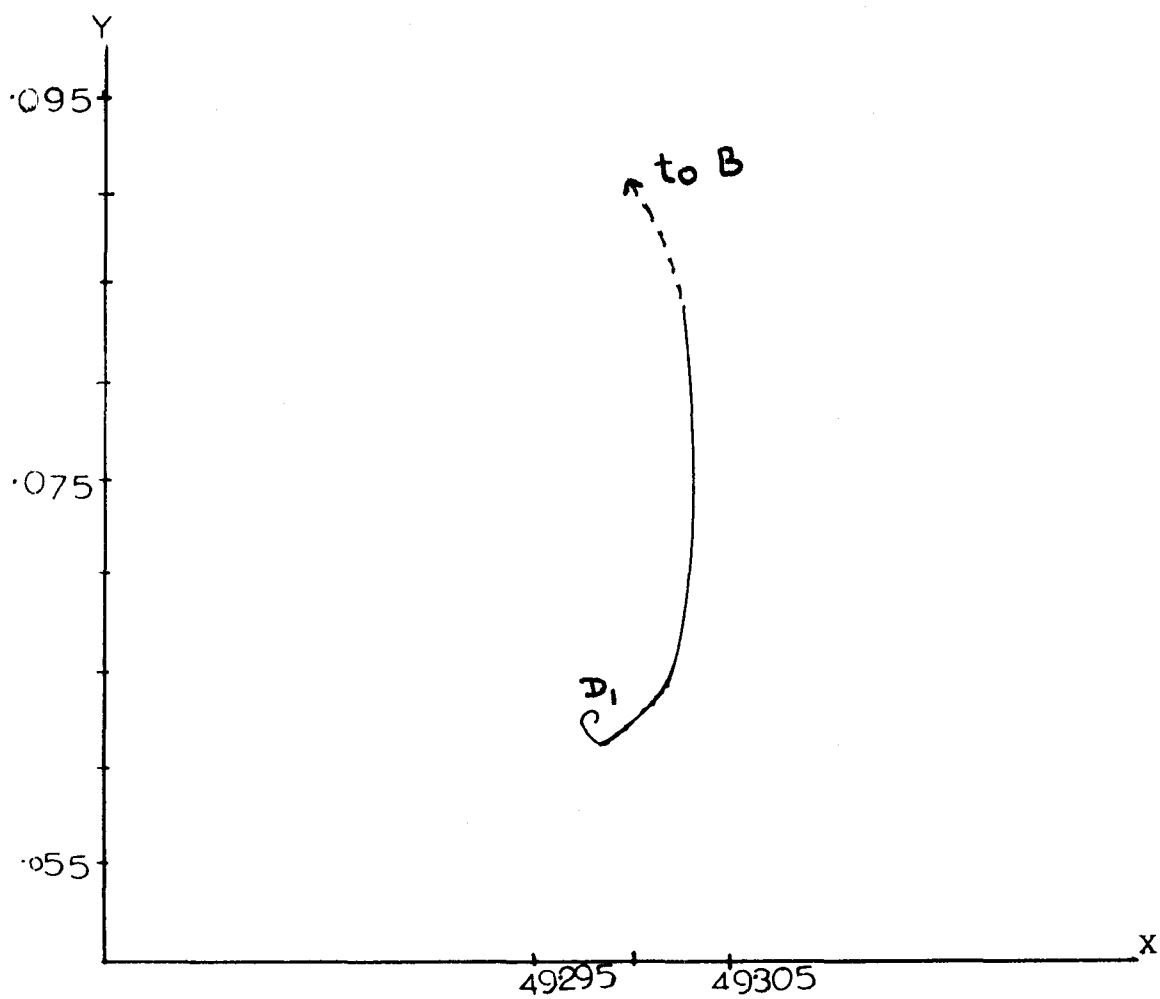


Fig. 18

The shape of upper spiral vortex for $\alpha = 15^\circ$ and $\sigma = 0.1$

No Gravity

$$\alpha = 10^\circ$$

$$C = 22.0g$$

$$C_L = 0$$

$$C_D = .073$$

$$\sigma = .1$$

Gravity $F^2 = 36$

$$C = 18.40$$

$$C_L = - .13$$

$$C_D = .0711$$

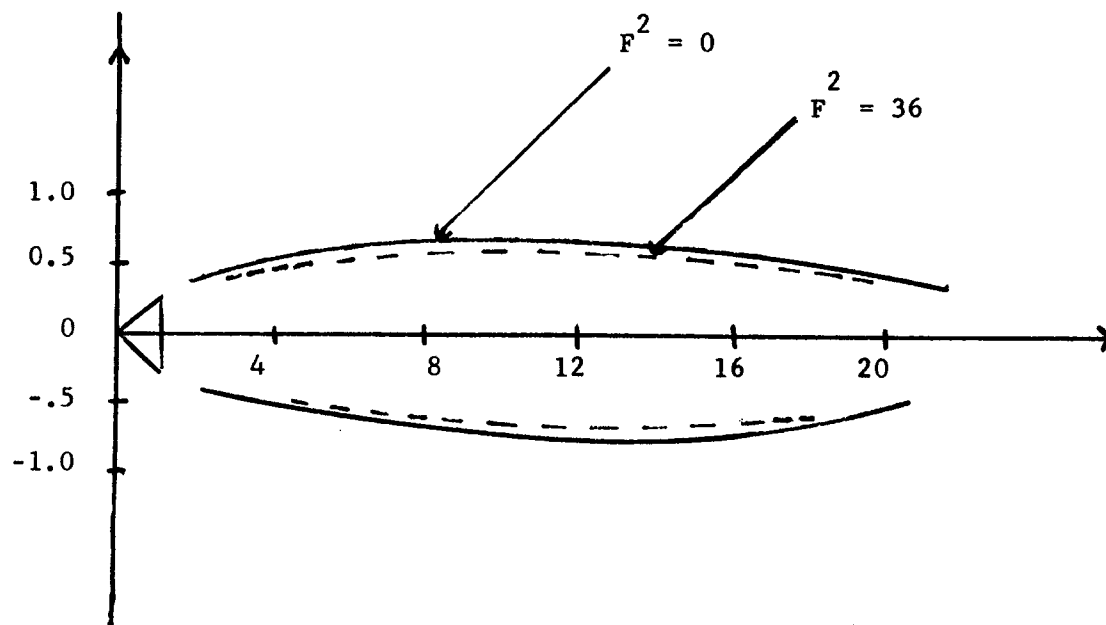


Fig. 19

The effect of Froude number ($F^2 = 36$) on the cavity shape shown by the broken lines.
The smooth lines show the cavity shape when $F^2 = 0$

No Gravity

$\alpha = 5^\circ$

$C = 5.74$

$C_L = 0$

$C_D = .0651$

$\sigma = .1$

Gravity

$F^2 = 16$

$C = 4.13$

$C_L = -.015$

$C_D = .0645$

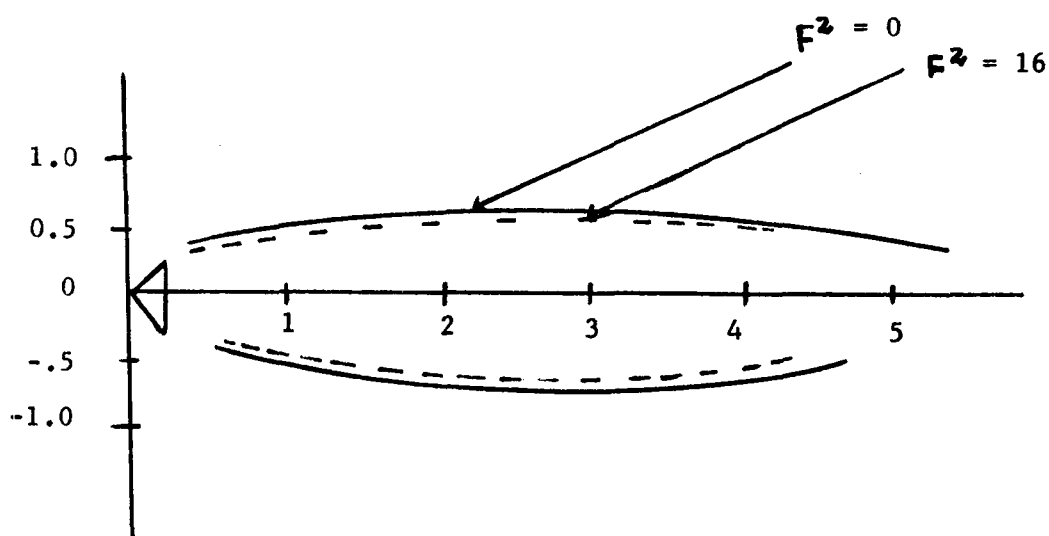


Fig. 20

The effect of Froude number ($F^2 = 16$) on the cavity shape shown by the broken lines.

The smooth lines show the cavity shape when $F^2 = 0$

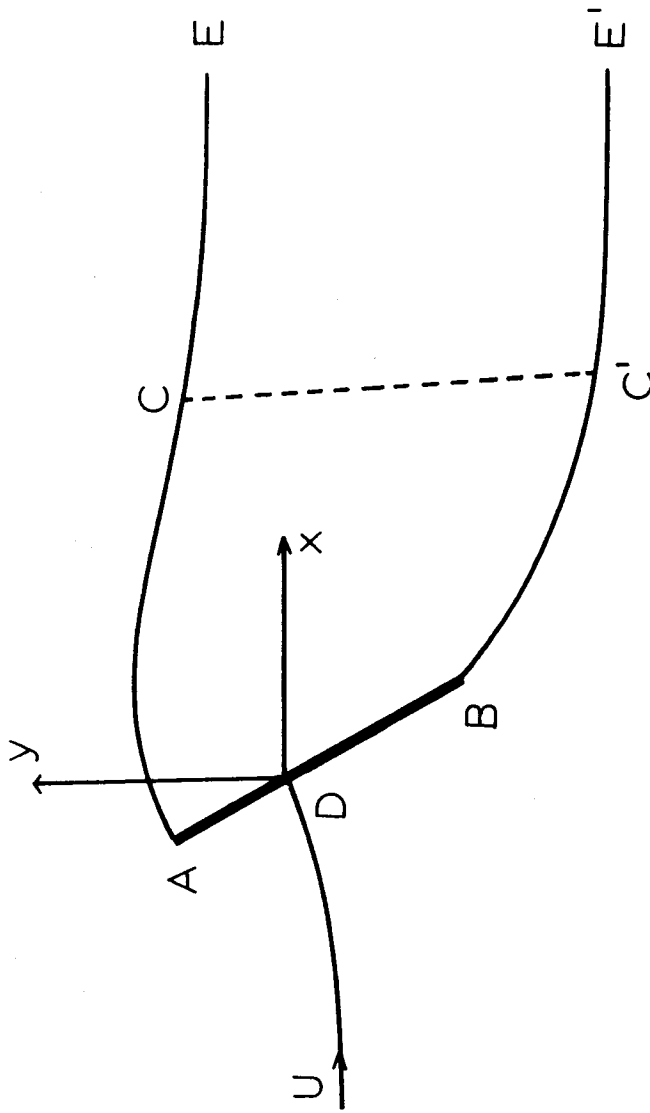


Fig. 21

Physical flow plane for fully cavitating flow (flat plate)

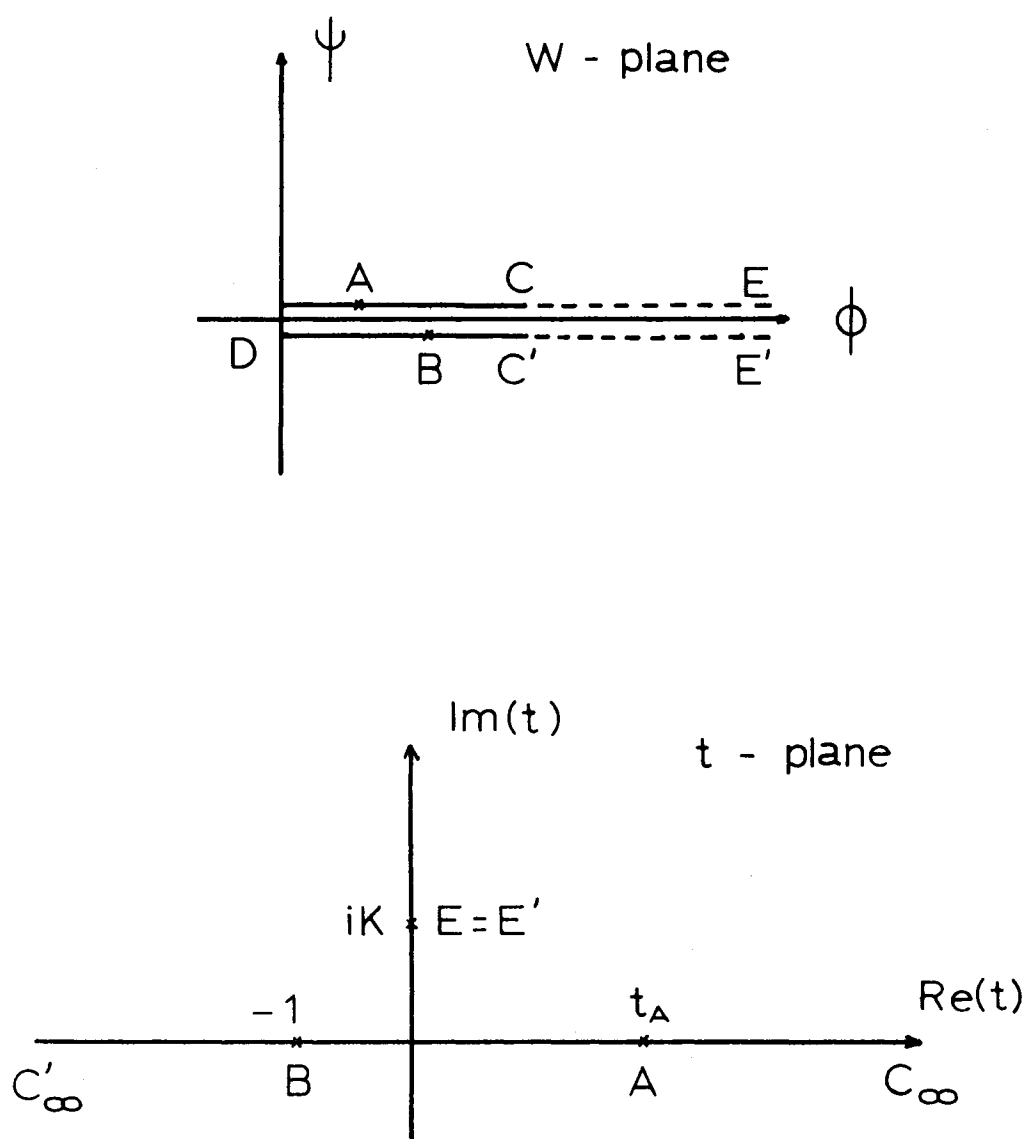


Fig. 22

Complex potential plane and parameter plane for fully cavitating flow (flat plate)

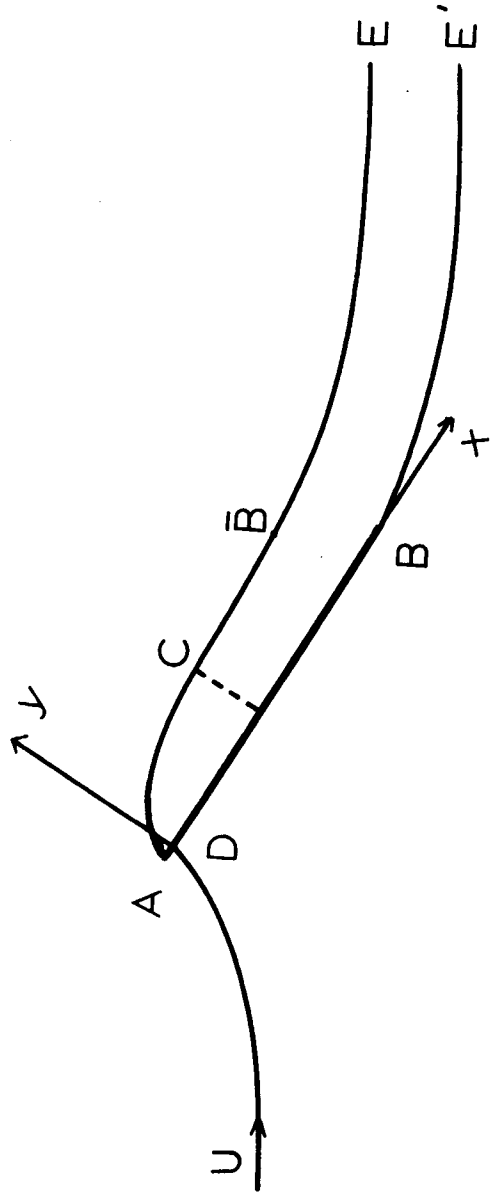


Fig. 23

Physical flow plane for partially cavitating flow

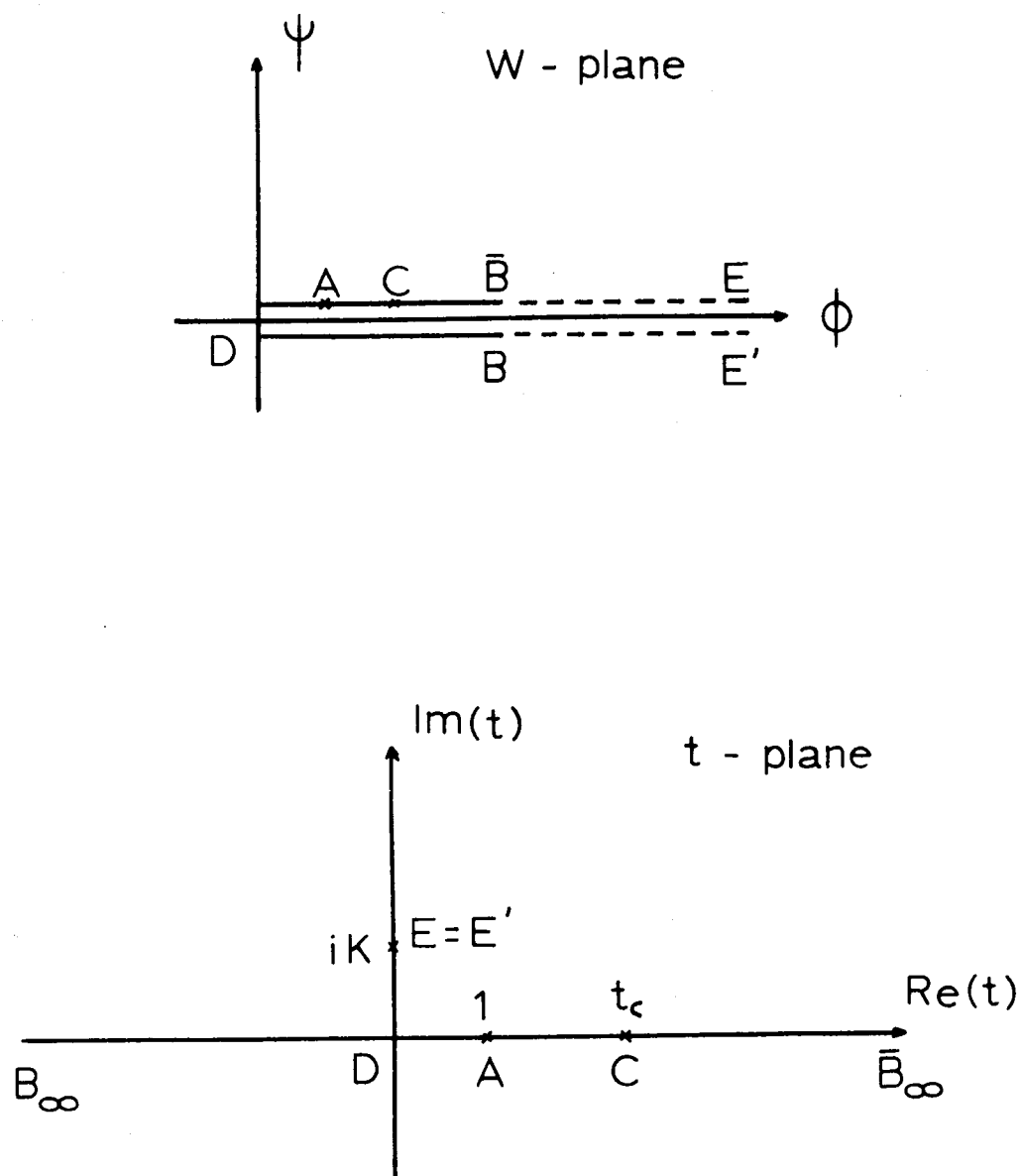


Fig. 24

Complex potential plane and parameter plane for partially cavitating flow

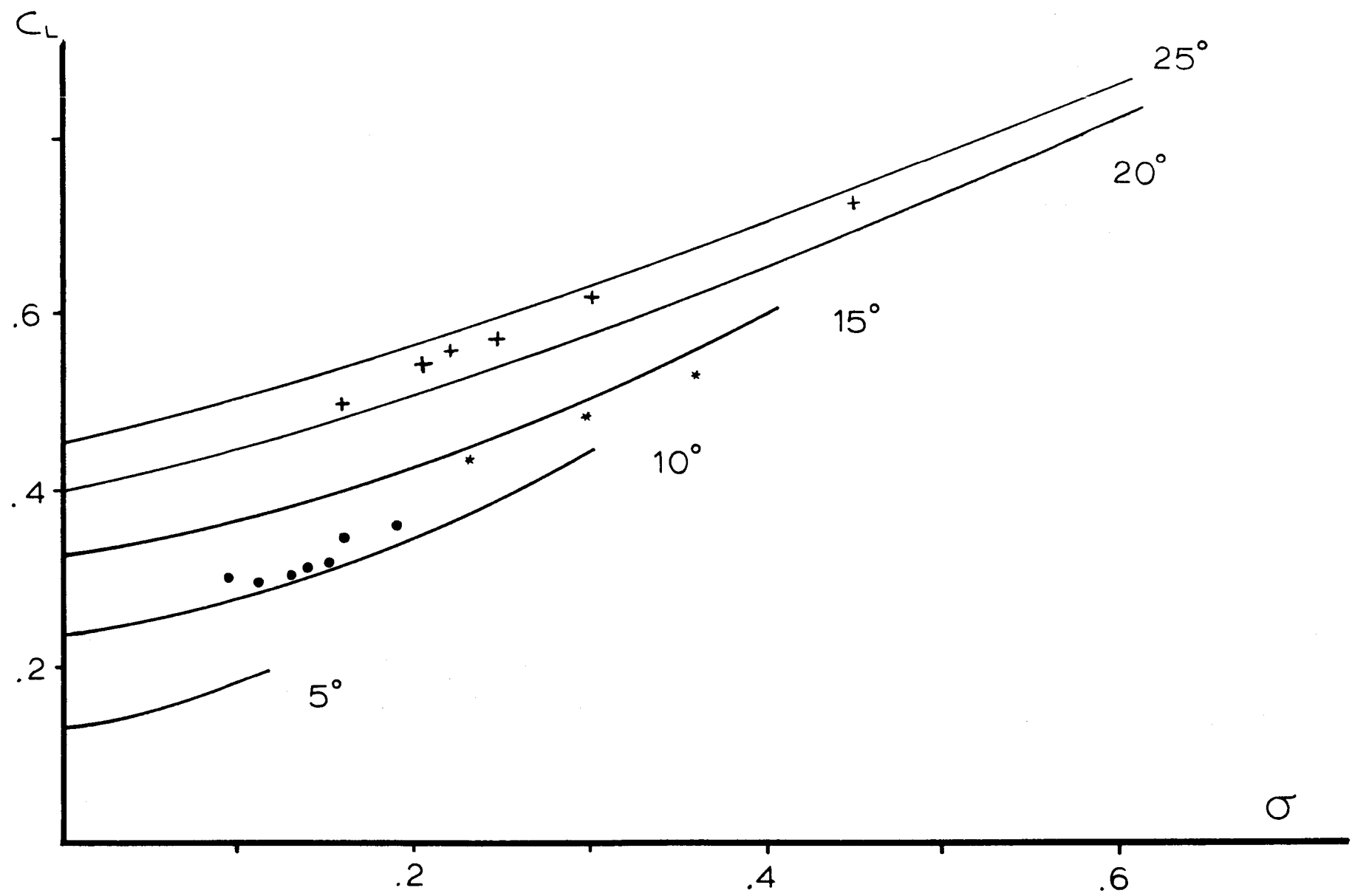


Fig. 25

Lift coefficient vs cavitation number for fully cavitating flow (flat plate). Experimental results of Parkin (*) for $\alpha = 15^\circ$, Silbermann (+) for $\alpha = 25^\circ$, and Dawson (•) for $\alpha = 10^\circ$ are included

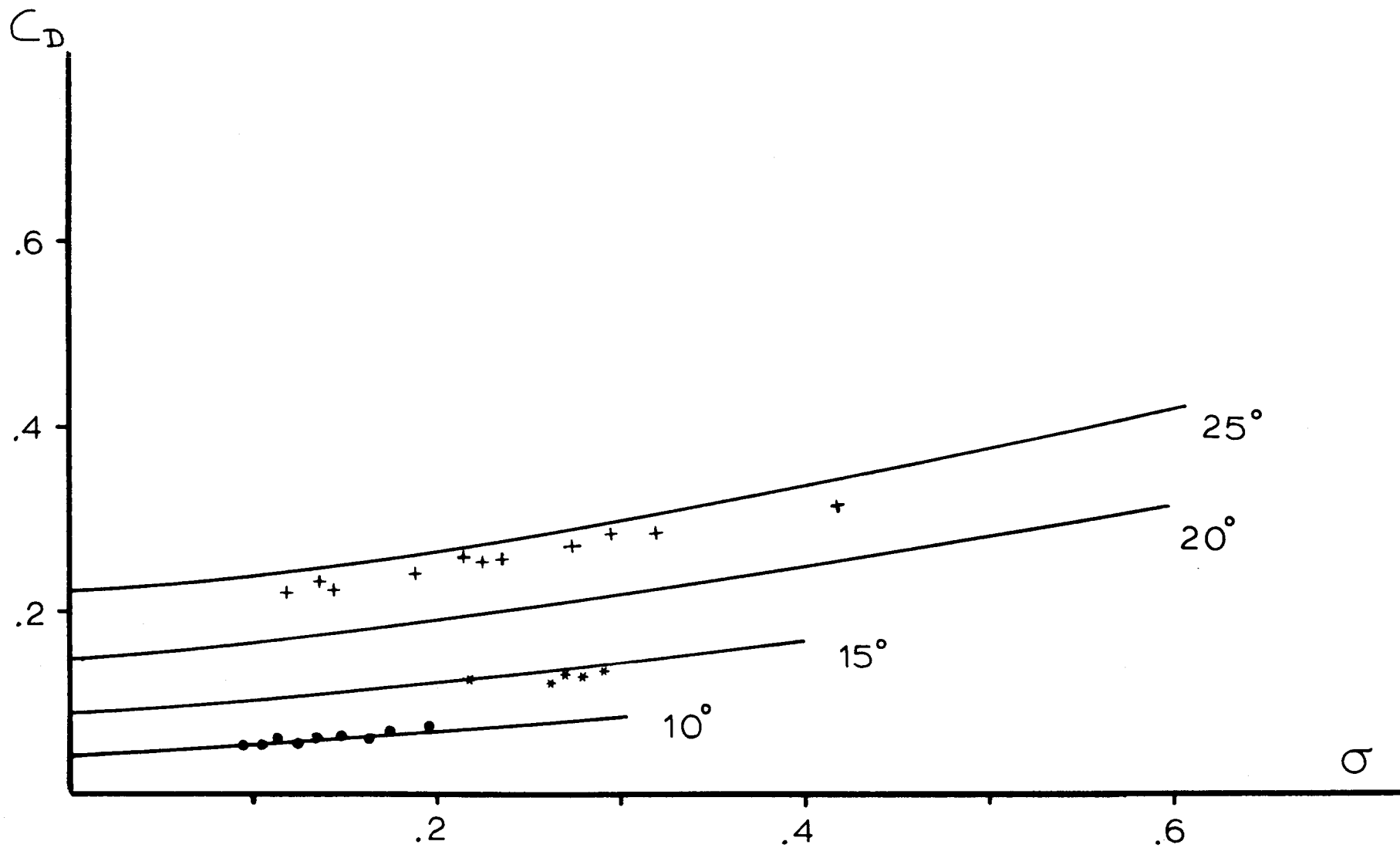


Fig. 26

Drag coefficient against cavitation number for fully cavitating flow (flat plate). Experimental results of Parkin (*) for $\alpha = 15^\circ$. Silbermann (+) for $\alpha = 25^\circ$, and Dawson (•) for $\alpha = 10^\circ$ are included

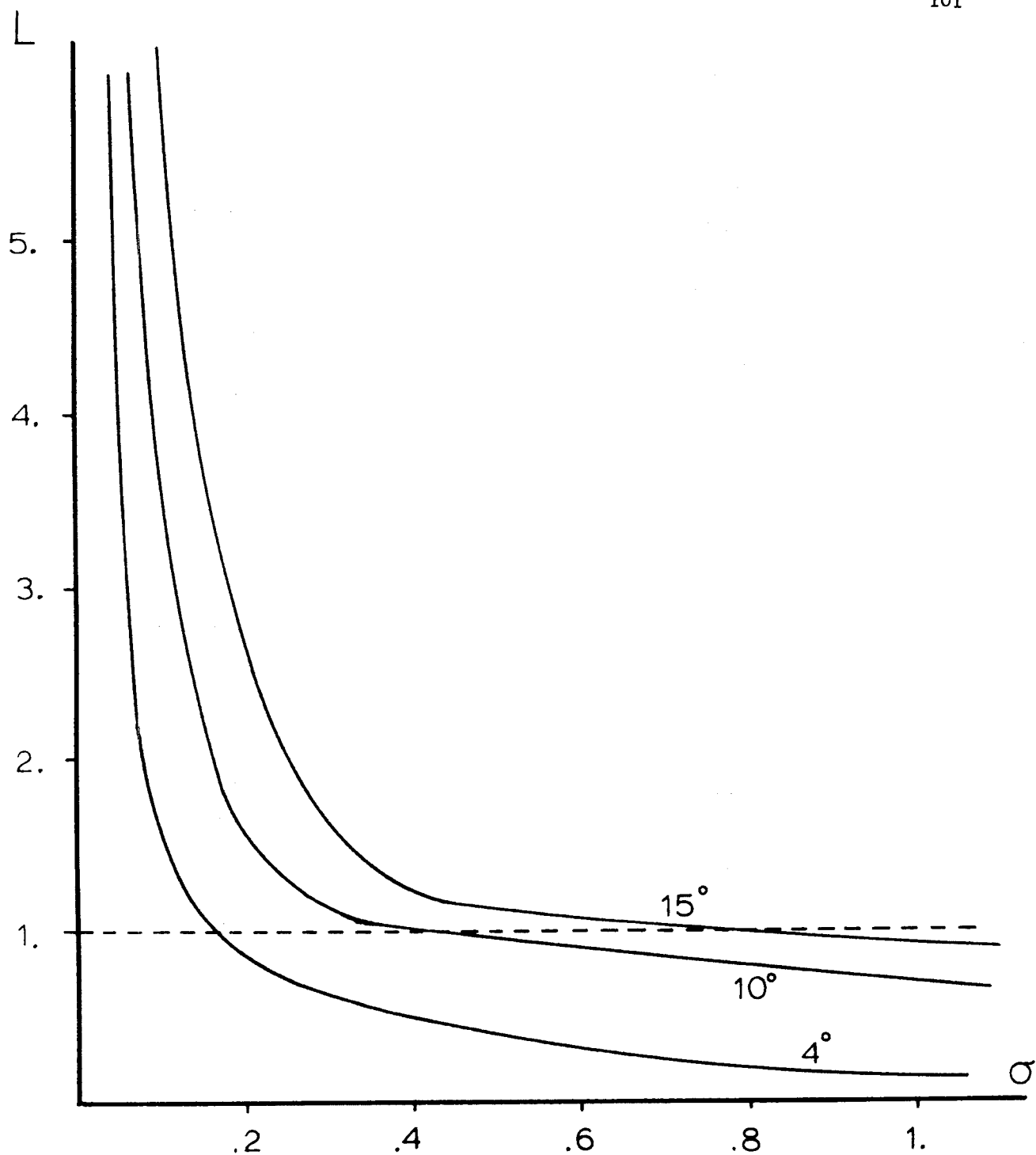


Fig. 27

Normalized cavity length against cavitation number. The horizontal line marks the transition between fully and partially cavitating regime

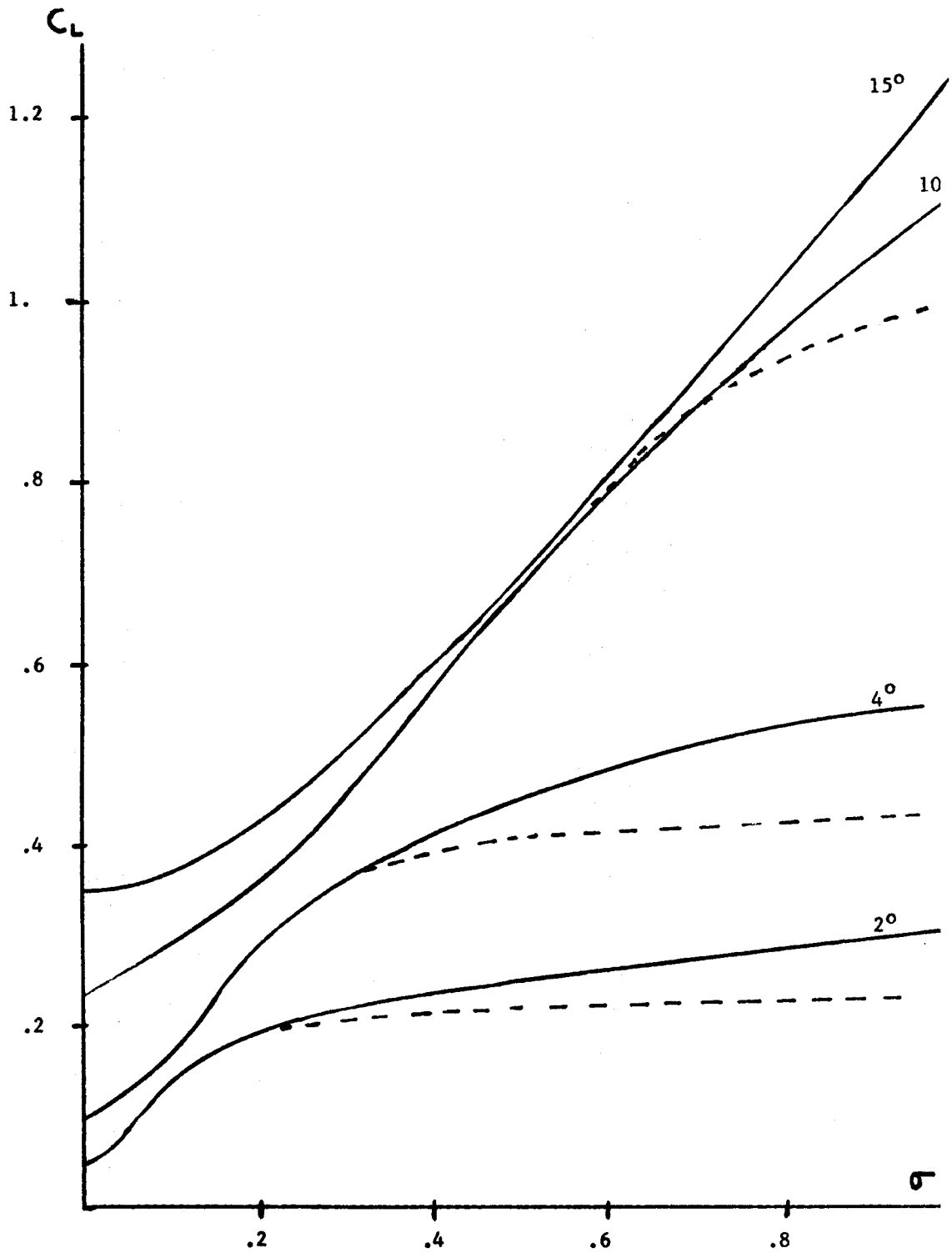


Fig. 28

Lift coefficient against cavitation number for flat plates, including both fully and partially cavitating regime. Dashed lines represent Wu's results.

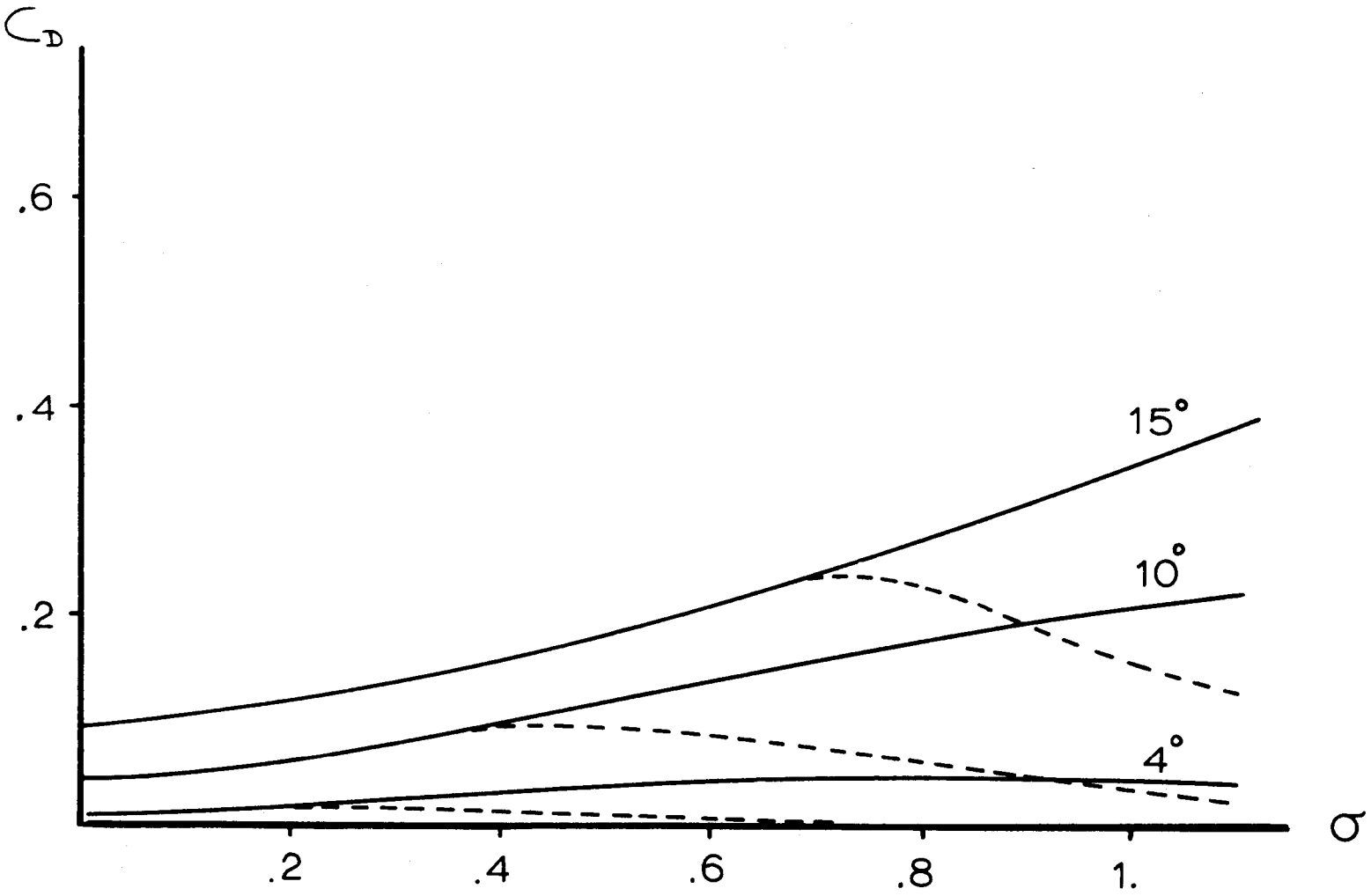


Fig. 29

Drag coefficient against cavitation number for flat plate, including both fully and partially cavitating regimes. Dashed lines represent Wu's results

VITA AUCTORIS

- 1942 Born in Mathura, U.P., India
- 1960 Graduated from Agra University, Agra, U.P., India, where I received my Bachelor of Science
- 1962 Received my Master of Science (Mathematics) from Agra University, Agra, U.P., India
- 1967 Received Master of Science (Mathematics) from University of Windsor, Windsor, Ontario, Canada
- 1969 Candidate for Doctor of Philosophy